USGS
science for a changing world

Prepared in cooperation with the
U.S. Department of Energy and the U.S. Department of Defense

MODFLOW-2000, THE U.S. GEOLOGICAL SURVEY MODULAR GROUND-WATER MODEL — DOCUMENTATION OF THE ADVECTIVE-TRANSPORT OBSERVATION (ADV2) PACKAGE, VERSION 2

Open-File Report 01-54

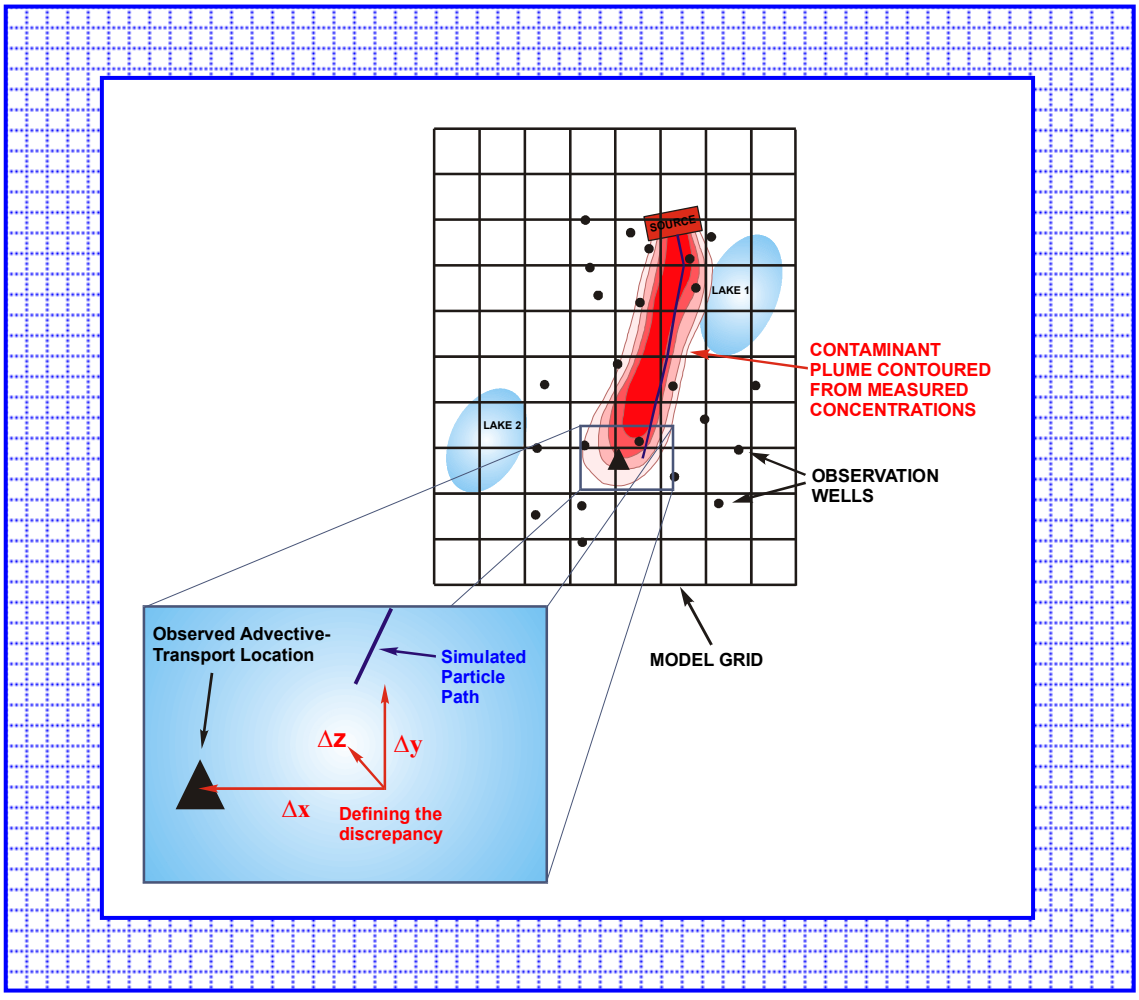

U.S. Department of the Interior
U.S. Geological Survey

MODFLOW-2000, THE U.S. GEOLOGICAL SURVEY MODULAR GROUND-WATER MODEL — DOCUMENTATION OF THE ADVECTIVE-TRANSPORT OBSERVATION (ADV2) PACKAGE, VERSION 2

By **Evan R. Anderman**[1] *and* **Mary C. Hill**[2]

U.S. Geological Survey

Open-File Report 01-54

Prepared in cooperation with the U.S. Department of Energy and the U.S. Department of Defense

Denver, Colorado
2001

---

[1] Calibra Consulting LLC, Denver, CO
[2] U.S. Geological Survey, Boulder, CO

U.S. DEPARTMENT OF THE INTERIOR
Gale A. Norton, *Secretary*

U.S. GEOLOGICAL SURVEY
Charles G. Groat, *Director*

For additional information write to:

Regional Research Hydrologist
U.S. Geological Survey
Box 25046, Mail Stop 413
Denver Federal Center
Denver, CO 80225-0046

Copies of this report can be purchased from:

U.S. Geological Survey
Branch of Information Services
Box 25286
Denver, CO 80225-0425

PREFACE

The computer program described in this report is designed to allow observations of the advective transport of steady-state ground-water flow through porous media to be used in the estimation of ground-water flow parameters. The program is developed as a package for MODFLOW-2000, the U.S. Geological Survey's three-dimensional ground-water flow parameter-estimation model. The documentation presented here includes brief listings of the methods used and detailed descriptions of the required input files and how the output files are typically used. This report supersedes Open-File Report 97-14, which documented ADV1, the version of this program that was compatible with MODFLOWP (Hill, 1992).

The code for this model is available for downloading over the Internet from a U.S. Geological Survey software repository. The repository is accessible on the World Wide Web from the U.S. Geological Survey Water Resources Information web page at URL http://water.usgs.gov/software/ground_water.html. The performance of the ADV2 Package has been tested in a variety of applications. Future applications, however, might reveal errors that were not detected in the test simulations. Users are requested to notify the U.S. Geological Survey of any errors found in this document or the computer program using the email address available on the website. Updates might occasionally be made to both this document and to the ADV2 Package, and users should check the website.

CONTENTS

FIGURES

TABLES

MODFLOW-2000, THE U.S. GEOLOGICAL SURVEY MODULAR GROUND-WATER MODEL — DOCUMENTATION OF THE ADVECTIVE-TRANSPORT OBSERVATION (ADV2) PACKAGE, VERSION 2

By Evan R. Anderman and Mary C. Hill

ABSTRACT

Observations of the advective component of contaminant transport in steady-state flow fields can provide important information for the calibration of ground-water flow models. This report documents the Advective-Transport Observation (ADV2) Package, version 2, which allows advective-transport observations to be used in the three-dimensional ground-water flow parameter-estimation model MODFLOW-2000. The ADV2 Package is compatible with some of the features in the Layer-Property Flow and Hydrogeologic-Unit Flow Packages, but is not compatible with the Block-Centered Flow or Generalized Finite-Difference Packages.

The particle-tracking routine used in the ADV2 Package duplicates the semi-analytical method of MODPATH, as shown in a sample problem. Particles can be tracked in a forward or backward direction, and effects such as retardation can be simulated through manipulation of the effective-porosity value used to calculate velocity. Particles can be discharged at cells that are considered to be weak sinks, in which the sink applied does not capture all the water flowing into the cell, using one of two criteria: (1) if there is any outflow to a boundary condition such as a well or surface-water feature, or (2) if the outflow exceeds a user specified fraction of the cell budget. Although effective porosity could be included as a parameter in the regression, this capability is not included in this package.

The weighted sum-of-squares objective function, which is minimized in the Parameter-Estimation Process, was augmented to include the square of the weighted x-, y-, and z-components of the differences between the simulated and observed advective-front locations at defined times, thereby including the direction of travel as well as the overall travel distance in the calibration process. The sensitivities of the particle movement to the parameters needed to minimize the objective function are calculated for any particle location using the exact sensitivity-equation approach; the equations are derived by taking the partial derivatives of the semi-analytical

particle-tracking equation with respect to the parameters. The ADV2 Package is verified by showing that parameter estimation using advective-transport observations produces the true parameter values in a small but complicated test case when exact observations are used.

To demonstrate how the ADV2 Package can be used in practice, a field application is presented. In this application, the ADV2 Package is used first in the Sensitivity-Analysis mode of MODFLOW-2000 to calculate measures of the importance of advective-transport observations relative to head-dependent flow observations when either or both are used in conjunction with hydraulic-head observations in a simulation of the sewage-discharge plume at Cape Cod, Massachusetts. The ADV2 Package is then used in the Parameter-Estimation mode of MODFLOW-2000 to determine best-fit parameter values. It is concluded that, for this problem, advective-transport observations improved the calibration of the model and the estimation of ground-water flow parameters, and the use of formal parameter-estimation methods and related techniques produced significant insight into the physical system.

INTRODUCTION

The use of nonlinear regression to estimate optimal parameter values of ground-water flow models (Yeh, 1986; Carrera and Neuman, 1986a, b, and c; Cooley and Naff, 1990; Hill, 1992; Sun, 1994) results in more objective, automated, model calibration than using trial-and-error calibration methods alone, and allows for quantitative evaluation of model reliability. Use of nonlinear regression also raises awareness of problems in ground-water flow model calibration that often are obscure when calibration is accomplished by trial and error alone. Such problems include (1) parameters important to the predictions for which the ground-water flow model is developed may not be precisely estimated because available observations provide insufficient information; (2) high correlation between parameters prevents them from being uniquely estimated using available observations, even though the individual parameter values may be important to predictions; and (3) different ground-water flow model constructions with optimal parameter estimates may fit the available observations equally well. Use of regression in the model calibration procedure makes these problems more obvious.

Historically, many ground-water flow models have been calibrated using only measurements of hydraulic head. The insensitivity and non-uniqueness that often occur when only head observations are used can be reduced by obtaining additional field observations, such as flow rate at head-dependent boundaries (Hill, 1992), prior information (Cooley, 1982; Cooley and Naff, 1990; Hill and others, 2000), temperature (Woodbury and Smith, 1988; Doussan and others, 1994), formation electrical resistivity (Ahmed and others, 1988), or concentration (Strecker and Chu, 1986; Wagner and Gorelick, 1987; Sun and Yeh, 1990a and b; Keidser and Rosbjerg, 1991; Cheng and Yeh, 1992; Weiss and Smith, 1993; Xiang and others, 1993; Sun, 1994; Christiansen and others, 1995; Harvey and Gorelick, 1995; Hyndman and Gorelick, 1996; Medina and Carrera, 1996; and others).

Using concentration data directly in the nonlinear regression is complicated by, among other things, the large computational effort required to solve the advective-dispersive solute-transport equation. Partly because of this problem, parameter-estimation models that use concentration data directly are not widely used in practice, effectively limiting the calibration of ground-water flow model parameters to the use of head, flow, and prior-information data alone. It is apparent, therefore, that there is a need for innovative methods to extract fundamental ground-water flow system information from concentration data without resorting to the use of the advection-dispersion equation.

The U.S. Geological Survey, in cooperation with the U.S. Department of Energy and the U.S. Department of Defense, developed the Advective-Transport Observation (ADV2) Package of MODFLOW-2000 as an alternative approach to using concentration data directly by deriving observations of the advective component of solute transport from concentration data, and using these observations in the estimation of ground-water flow parameters. Observations of time and path of advective transport contain important information about ground-water flow parameters because these observations are a direct consequence of ground-water velocities and generally reflect long-term aquifer conditions more than do observations of head or flow.

Accurately locating the advective front of a contaminant plume directly from concentration data can be difficult because of the effects of, for example, transverse dispersion and complex patterns of transport. Some of the difficulties are investigated in this report using synthetic test cases. Use of advective-transport observations in the estimation of ground-water flow parameters in field problems was considered by Sykes and Thomson (1988) and Anderman and others (1996). Both concluded that the advective-transport observations were important to model calibration.

Purpose and Scope

This report documents the Advective-Transport Observation (ADV2) Package of the three-dimensional ground-water flow parameter-estimation model MODFLOW-2000 (Harbaugh and others, 2000; Hill and others, 2000). Advective-transport observations are compared to particle paths simulated using particle-tracking methods. The weighted sum-of-squares objective function of MODFLOW-2000 is augmented to include the square of the weighted x-, y-, and z-components of the differences between the simulated and observed advective-transport locations at defined times. This method expands on the work of Sykes and Thomson (1988) by using the position of advective transport as well as the overall travel time. The particle-tracking capabilities of the ADV2 module are evaluated using the sample problem presented in the MODPATH documentation by Pollock (1994, p. 6-1). Using advective-transport observations to estimate parameter values is evaluated in a small but complex synthetic test case. The use of advective-transport observations in a field problem is demonstrated through an application to the Otis Air Force Base sewage-discharge plume on Cape Cod, Massachusetts. Input and output of the ADV2 Package are presented in appendix A; derivation of the sensitivity equations is presented in appendix B; the program structure is described in appendix C.

Conceptual Approach

The conceptual basis for the use of advective-transport observations is best illustrated through an example of a hypothetical field area, as shown in figure 1. At this site, the contaminant source has been active long enough to produce an extensive plume. A number of monitoring wells measure the extent of contaminated ground water, as well as the elevation of the water table. Additionally, the average annual amount of flow between one of the lakes and the ground-water system has been measured. The sharp fronts of the concentration contours shown in figure 1 indicate that the movement of the contaminant plume is largely due to advection so that the direction and length of the plume are controlled by the hydrogeologic characteristics of the field site. Although the head and flow observations represent aquifer conditions at discrete points in time, the configuration of the contaminant plume represents average aquifer conditions integrated over the time of contaminant movement. An advective-transport observation can be obtained by contouring measured contaminant concentrations and choosing a suitable point along the plume front, as shown by the triangle in figure 1. The selection of the advective-front location is generally not straightforward and is discussed in more detail in the Obtaining Advective-Transport Observations section. Once an observation is obtained, a simulated equivalent is needed. To simulate advective transport, a particle is tracked through the grid from the source location for the total time of contaminant transport, as shown by the gray line in figure 1. The differences in the x-, y-, and z-components between the simulated and observed advective-front locations are then used in the nonlinear regression in conjunction with the differences between the simulated and observed heads and flows to estimate model parameter values. The ADV2 Package also supports backward particle tracking. In the example shown in figure 1, a particle would be introduced at the final position of the plume front and tracked backward toward the source.

There are several conceptual and practical advantages of particle tracking over the use of the full advection-dispersion equation. First, particle tracking is not affected by numerical dispersion, which hampers many advection-dispersion models (Zheng and Bennett, 1995; Mehl and Hill, 2000; Mehl and Hill, 2001). Second, the computational effort is greatly reduced

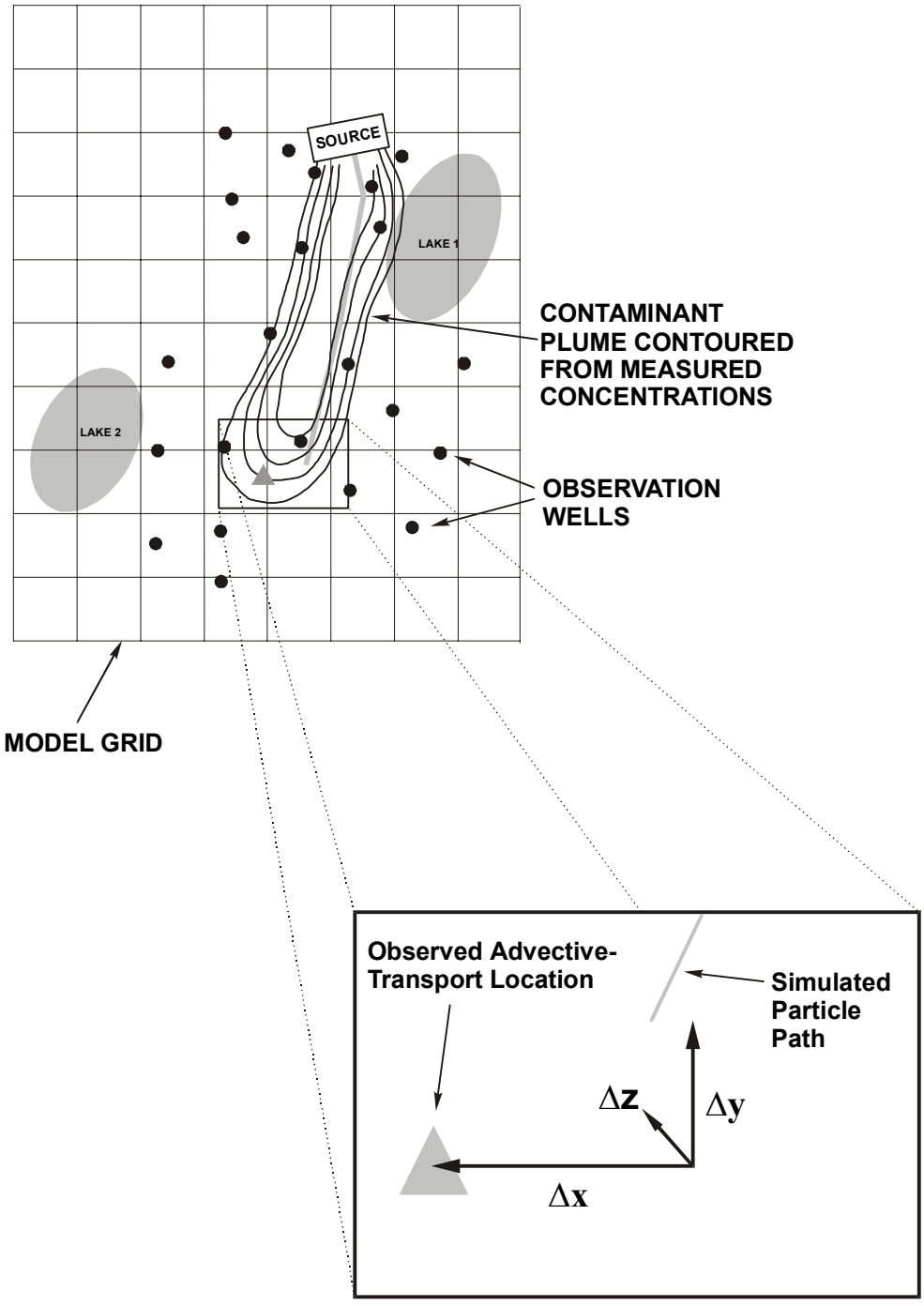

Figure 1. Conceptual representation of advective-transport observations.

because computations are required only along the particle path. Only a single particle usually needs to be tracked to represent the advective transport of each point source considered.

Particle tracking has at least two primary drawbacks. First, it is unclear how to locate the advective front of a contaminant plume or age-dated water moving in three dimensions in the presence of dispersion, retardation, decay, chemical reactions, a possibly transient flow field, and other factors that cause subsurface transport in actual systems to differ from plug flow. In many instances, these problems are compounded by the absence of a reliable history of source release times, strengths, amounts, or locations. Some comments about these problems are presented in the Obtaining Advective-Transport Observations section. Even if the advective-transport location is characterized by typical errors, however, many flow models would benefit from quantitative consideration of available information on flow direction and rate.

The second drawback to the use of particle tracking is that abrupt lateral or vertical changes in hydraulic conductivity can result in simulated flow paths that change dramatically as hydraulic conductivity changes (LaVenue and others, 1989; Poeter and Gaylord, 1990). These dramatic changes can violate smoothness requirements of gradient-based optimization methods, such as the modified Gauss-Newton method used in MODFLOW-2000. An example of this problem is presented in the Common Problems section. Severe situations can diminish the utility of sensitivity analyses and optimization methods such as those described by Hill (1998).

As mentioned above, the time and path of travel also could be determined from a tracer test or from age dating of water samples that originate from a known location. The model presented here is applicable to these and many other situations, but is not applicable to situations in which the source or destination location is unspecified.

Methods

To incorporate particle tracking into the modified Gauss-Newton optimization method used in MODFLOW-2000, the calculated particle location and its sensitivity to each estimated parameter are needed. Particle location is simulated by tracking the successive Cartesian (x-, y-, and z-) components of particle displacement through the ground-water flow model grid over time. Particle tracking was incorporated into the Observation, Sensitivity, and Parameter-Estimation Processes of MODFLOW-2000 for particles moved by steady-state simulated flow. Particle-tracking computations are only required to determine the path of a single particle for each observation, greatly reducing the computational effort compared to solution of the advection-

dispersion equation. The particle-tracking method used is the semi-analytical method presented by Pollock (1989) modified so that the cell-face velocities are calculated using an interpolated saturated thickness instead of the single-cell saturated thickness used in MODPATH. The original method produces discontinuities in velocity, and thus in sensitivity, at cell boundaries. The velocity at any point within a cell is linearly interpolated from cell-face velocities. Users are allowed to track particles in a backward direction, and manipulation of the effective-porosity value needed to calculate velocity allows effects such as retardation to be simulated. Given an initial particle position, the x-, y-, and z-displacements are calculated and a single particle is tracked through the model grid for a specified amount of time. Particles can be discharged at cells that are considered to be weak sinks, in which the sink applied does not capture all the water flowing into the cell, using one of two criteria: (1) if there is any outflow to a boundary condition such as a well or surface-water feature, or (2) if the outflow exceeds a user specified fraction of the cell budget. The sensitivities of the particle movement to the parameters are calculated for any particle location using the exact sensitivity-equation approach, which is consistent with the sensitivity calculations in MODFLOW-2000, by taking the partial derivatives of the semi-analytical particle-tracking equation with respect to the parameters.

Acknowledgments

The authors acknowledge Pat Tucci, Brian Wagner, Dick Cooley, John Flager, Ned Banta, and Claire Tiedeman of the U.S. Geological Survey for their helpful technical reviews.

ADVECTIVE-TRANSPORT OBSERVATION PACKAGE METHODOLOGY

This section describes how the ADV2 Package incorporates advective-transport observations in the Observation, Sensitivity, and Parameter-Estimation Process of MODFLOW-2000. The discussion includes the complete derivation of the augmented weighted sum-of-squares objective function, a brief description of how sensitivities are calculated, and a brief description of the forward particle-tracking equations used in the ADV2 Package; complete derivations of the particle-tracking equations and sensitivities are presented in appendix B.

Augmented Objective Function and Normal Equations and the Calculation of Sensitivities

The ADV2 Package augments arrays in MODFLOW-2000 that may already contain observed and simulated hydraulic heads and flows and calculated observation sensitivities. In this way, the weighted sum-of-squares objective function in MODFLOW-2000 is augmented to include the square of the weighted x-, y-, and z-components of the difference between the simulated and observed advective-front location at defined times. The sum-of-squares objective function, S, is then expressed as:

$$\mathrm{S} = S_h + S_f + S_p + S_t \tag{1}$$

where

S_h is the sum of the squared weighted hydraulic-head differences,
S_f is the sum of the squared weighted head-dependent flow differences,
S_p is the sum of the squared weighted prior-information differences,
S_t is the sum of the squared weighted advective-transport differences, expressed as

$$\sum_{i=1}^{NT} \omega_i \left(x_i - \hat{x}_i\right)^2 + \upsilon_i \left(y_i - \hat{y}_i\right)^2 + \tau_i \left(z_i - \hat{z}_i\right)^2 \tag{1a}$$

where

NT is the number of advective-transport observations,
x_i, y_i, z_i are the x-, y-, and z-components of the observed advective transport,
$\hat{x}_i, \hat{y}_i, \hat{z}_i$ are the x-, y-, and z-components of the simulated advective transport, and
$\omega_i, \upsilon_i, \tau_i$ are the x-, y-, and z- advective-transport observation weights.

The above expression for S_t is applicable when the weight matrix is diagonal, indicating that covariances between measurement errors are ignored. Although this is common in practice, the

ADV2 Package supports a full weight matrix, as discussed in appendix A. While errors in the x-, y-, and z-advective-transport movements are probably not independent, how to determine error correlation is not clear, and few users are expected to use a full weight matrix. In the following discussion, a diagonal weight matrix is assumed.

Determination of proper weighting is nearly always problematic. Linear theory indicates that parameter estimates with the smallest variances are achieved when the weights of equation 1a equal the inverses of variances of the observation measurement error (Graybill, 1976; Draper and Smith, 1981, p. 110; Hill, 1998); the authors have found this to be a useful guideline for nonlinear problems as well (Hill, 1998; Hill and others, 1998). Standard deviations and coefficients of variation are more intuitive to work with than are variances and can be used to calculate variances as the square of the product of the coefficient of variation and the measured value, or the square of the standard deviation. The ADV2 Package allows the user to choose what type of statistic will be listed in the input file.

The minimum of the objective function in equation (1) is determined using the modified Gauss-Newton nonlinear optimization procedure presented by Hill (1998, p. 8, eq. 4):

$$\begin{aligned} \left(\underline{C}^T\left(\underline{X}_r^T\,\underline{\hat{\omega}}\,\underline{X}_r+\underline{R}\right)\underline{C}+\underline{I}\mu_r\right)\underline{C}^{-1}\,\underline{d}_r &= \underline{C}^T\,\underline{X}_r^T\,\underline{\hat{\omega}}\left(\underline{y}-\underline{\hat{y}}_r\right) \\ \underline{b}_{r+1} &= \underline{b}_r+\rho_r\,\underline{d}_r \end{aligned} \qquad (2)$$

where

$\underline{C}$ is a diagonal scaling matrix with elements equal to
$C_{ii}=\left(\underline{X}_r^T\,\underline{\hat{\omega}}\,\underline{X}_r\right)_{ii}^{-1/2};\quad C_{ij}=0, i\neq j$

$\underline{X}_r$ is the sensitivity matrix evaluated at parameter values $\underline{b}_r$, with column j equal to $\frac{\partial\underline{\hat{y}}_r}{\partial b_j}$, where b_j is an element of $\underline{b}_r$.

r is the parameter-estimation iteration number,

$\underline{\hat{\omega}}$ is the weight matrix,

$\underline{R}$ can be included for problems with large residuals and a large degree of nonlinearity (see Hill, 1998, p. 78),

$\underline{I}$ is the identity matrix, with elements equal to 1 along the diagonal and zero elsewhere,

μ_r is the Marquardt parameter,

$\underline{d}_r$ is the vector used to update the parameter estimates,

$\underline{y}$ is the vector of observed values, such as heads, flows, and prior information,

$\underline{\hat{y}}_r$ is the vector of corresponding simulated values,

ρ_r is the damping parameter, and

T superscript indicates the transpose of the vector or matrix.

To include advective-transport observations in the parameter estimation, $\underline{y}$, $\underline{\hat{y}}_r$, $\underline{\hat{\omega}}$, and $\underline{X}_r$ of the normal equations are augmented as follows. The advective-transport observation values are added to the observations in vector $\underline{y}$, which becomes:

$$\underline{y} = \begin{pmatrix} y_1 \\ \vdots \\ y_{nh} \\ y_{nh+1} \\ \vdots \\ y_{nh+nq} \\ y_{nh+nq+1} \\ \vdots \\ y_{nh+nq+nt*ktdim} \\ p_1 \\ \vdots \\ p_{npr} \end{pmatrix} \tag{3}$$

where

nh is the number of head observations,

nq is the number of flow observations,

nt is the number of advective-transport observations,

ktdim is the dimension of the particle tracking (either 2 or 3),

p_i is the prior estimate on a parameter, and

npr is the number of prior estimates on the parameters.

The corresponding simulated-equivalent values are calculated using the particle-tracking equations of the following sections and are added to the simulated-value vector $\underline{\hat{y}}_r$ at each parameter-estimation iteration. Thus, $\underline{\hat{y}}_r$ looks similar to $\underline{y}$ of equation (3) except that the elements are simulated instead of observed values. The weights of each of the advective-transport observations are added to the weight matrix $\underline{\hat{\omega}}$. Thus, the augmented $\underline{\hat{\omega}}$ is a nh+nq+nt*ktdim+npr dimensional square matrix of the form shown by Hill (1998, p. 77). The sensitivity matrix $\underline{X}_r$ is augmented with the sensitivity of the advective-transport simulated values *i* to each parameter *j*. The parameter vector $\underline{b}_r$ remains unchanged.

Calculation of sensitivities is the most computationally intensive part of nonlinear regression. Depending on the number of observations and estimated parameters, there are more and less efficient methods to numerically calculate the sensitivities. The sensitivity-equation method (Yeh, 1986) is most efficient when the number of observation locations exceeds the number of estimated parameters and is the only method supported by MODFLOW-2000 and the ADV2 Package. Sensitivity-equation sensitivities for advective travel are calculated using the sensitivity-equation sensitivities of hydraulic head throughout the grid calculated by the Sensitivity Process (Hill and others, 2000). The equations for advective-transport sensitivities are derived and presented in appendix B.

Calculation of Particle Location

Particle location is simulated by tracking the successive Cartesian (x-, y-, z-) components of particle displacement through the ground-water flow model grid either forward or backward in time. The derivations of the particle-tracking equations are given in appendix B for the x-component only; extension to the y- and z-components is straightforward. Vertical particle displacement is corrected for distorted grids using the methods of Pollock (1989, p. 12) and Zheng (1994). If the particle is discharged from the model grid before the time of the observation, the final simulated particle position is determined by projecting the particle using the velocities calculated at the point of discharge. Such projection of the final particle position often results in large advective-transport differences in equation 1, in effect penalizing advective transport of particles that exit the grid too soon.

The particle-tracking time-step size can be calculated several ways. Using the first option, particles are tracked from cell face to cell face using the semi-analytical particle-tracking approach, and the time-step size is calculated automatically and will vary from cell to cell. Using the second option, particles are displaced using a specified time-step size. In both cases, the particle position is printed to the output file for each particle step. Using the third option, the particle is tracked from cell face to cell face using a specified time-step size. If the time step is reached in between cell faces, the particle is displaced to that position, which is printed to the output file.

Particles are discharged at cells that have a strong sink term, where all of the cell-face velocities are into the cell. For weak-sink cells, where a sink is present but is not strong enough for all the velocities to point into the cell, there are two options for discharging particles. Particles

can be discharged at any weak-sink cell or, alternatively, only at cells where the sink size is larger than a specified fraction of the total cell flow.

Particles can be tracked in a backward direction in the ADV2 Package, a feature which has many uses in parameter estimation. For example, if the age of water at one point in the system and the likely source area are known, this feature can be used to represent the observation. Additionally, this feature can be used to calculate predicted well capture areas and the corresponding confidence intervals.

There are a number of special considerations that apply to the calculation of the vertical velocities that are worth discussing here. A nonzero vertical velocity at the top of the top layer can only occur if there is an appropriate boundary condition active in the cell. In MODFLOW-2000, a number of different types of boundaries, such as recharge, head-dependent boundaries (River, Streamflow-Routing, Drain, and General-Head Boundary Packages), and evapotranspiration, may contribute to the net flux at the top boundary. Conceptually, boundaries may represent sources of water that overlie, are adjacent to, or underlie the ground-water system being represented. Distinguishing these special cases is not necessary in MODFLOW-2000; however, the different conceptual representations of boundaries are important to particle tracking (Pollock, 1989, p. 15). While MODPATH allows the user to specify the cell face affected by an imposed boundary condition, the ADV2 Package supports a more limited representation of boundary flows. In the ADV2 Package, influx from boundary conditions that are applied to the top layer are assumed to apply to the top of the top layer. All other boundaries are considered as internal sources of water, so that the flow is assumed to be introduced at the cell center.

The finite-difference approximation equations upon which MODFLOW-2000 is based assumes that hydraulic properties are uniform within individual cells, or at least that average or integrated parameters can be specified for every cell (Harbaugh and others, 2000, p. 25). Hydraulic head is calculated at cell centers, so that hydraulic properties of adjacent cells need to be combined to calculate conductances to be used in the continuity equation. This is accomplished within MODFLOW-2000 for both the row and column components of horizontal conductance within layers as well as for the vertical hydraulic conductance between layers. Confining layers can be represented in the Layer-Property Flow (LPF) Package using the quasi-three-dimensional (quasi-3D) approach (Harbaugh and others, 2000). Confining units represented in this way do not require a separate layer in the finite-difference grid; however, their top and bottom elevations are defined in the discretization file. The particle-tracking algorithm presented here is capable of tracking particles through model layers and quasi-3D confining

layers, if present. If the simulation of transport in a confining unit is to include a horizontal component, however, the confining unit must be represented by one or more model layers and not as a quasi-3D confining unit. The ADV2 Package is not compatible with all of the flow and boundary-condition packages that formulate the finite-difference equations, as discussed in the Compatibility with MODFLOW-2000 Packages section of this report.

For three-dimensional applications, MODFLOW-2000 is capable of allowing distorted finite-difference grids that vary in thickness and elevation over the model area. While distortion of the model grid may better represent the flow system, error into the vertical tracking of a particle through the grid can be introduced if the track does not account for this distortion. An example of a distorted grid is shown in figure 2. The correction implemented in this work is based on the methodology of Pollock (1989, p. 12-14) and Zheng (1994), in which particles are tracked from cell face to cell face and the vertical position of a particle is corrected each time the particle moves from one cell to another within a given layer. The correction is calculated such that the ratio of the vertical distance of the particle from the bottom of the cell divided by the vertical length of the cell face is the same for adjoining cell faces.

Comparison of ADV2 to MODPATH Particle Tracking

To demonstrate that the implementation of the particle tracking procedure in ADV2 is correct, results are compared to published results of MODPATH (Pollock, 1989). The MODPATH sample problem consists of an unconfined aquifer separated from an underlying confined aquifer by a 20-ft thick confining layer (fig. 3). A partially penetrating well located in the center of the confined aquifer discharges at a rate of 80,000 cubic feet per day. The boundary conditions consist of (1) uniform areal recharge of 0.0045 foot per day to the unconfined aquifer; (2) no flow on all sides and along the bottom of the confined aquifer; and (3) a partially penetrating river located along one side at the top of the unconfined aquifer. The model grid consists of 27 rows and columns and 5 layers. Grid spacing varies from 40 ft by 40 ft at the well to 400 ft by 400 ft along the model edges. The unconfined aquifer is represented by layer 1 and

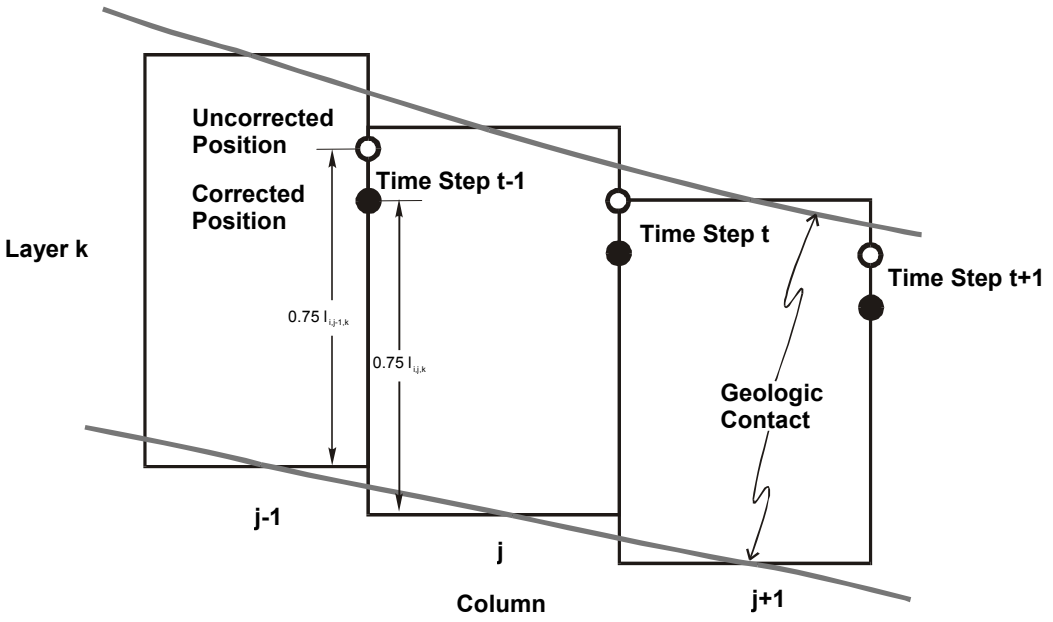

Figure 2. Correction to vertical particle position needed for distorted grid representing a sloping and restricting aquifer (modified from Zheng, 1994).

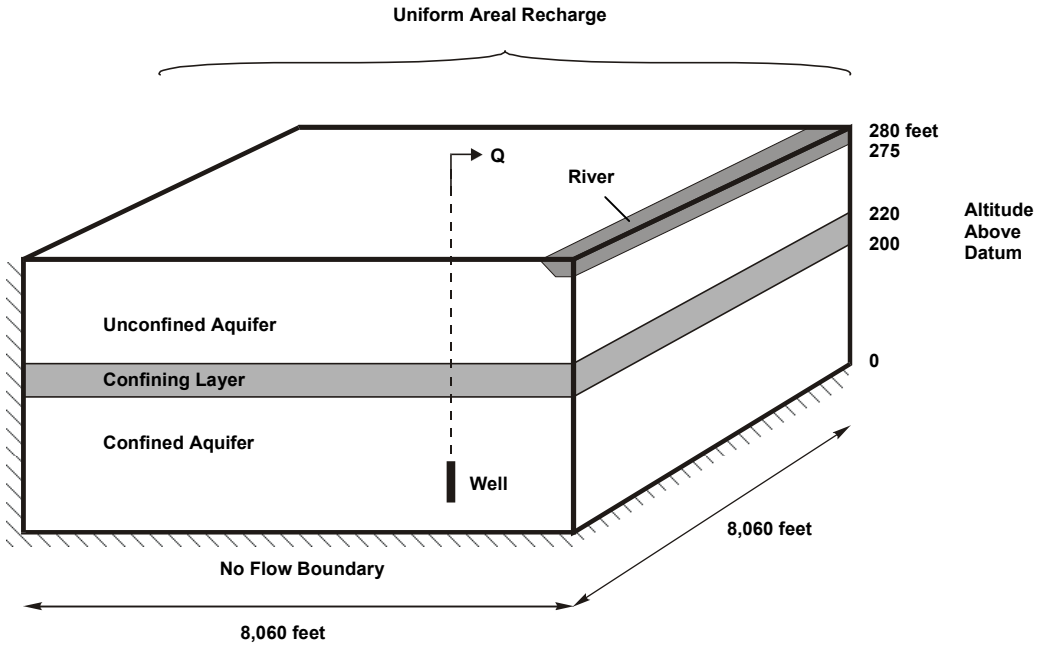

Figure 3. MODPATH sample problem (modified from Pollock, 1989).

has a variable thickness of approximately 80 ft. The confined aquifer is represented by four 50-ft thick layers, with the confining layer represented using the quasi-3D approach.

Many of the features included in MODPATH that populate the model grid with particles are not necessary for the particle tracking included in the ADV2 package, and reproducing all of the results demonstrated in the MODPATH sample problem is beyond the scope of this report. Comparison of the path lines for a cross section taken perpendicular to the river sufficiently demonstrates that the ADV2 particle tracking duplicates that of MODPATH. The path lines shown in figure 4 were generated using backward tracking from the well located in the cell at row 14 and column 14 of layer 4. Figure 4A was generated by MODPATH and is duplicated from Pollock (1989); Figure 4B was generated using the ADV2 package. The circles plotted in figure 4 represent the particle locations in 20-year increments starting from the well; thus, in both cases, the particles are tracked backwards. The two figures are almost identical, indicating that the particle-tracking algorithm included in ADV2 duplicates MODPATH.

The particle-location sensitivities to the parameters calculated by the ADV2 Package using the methodology presented here were tested in a variety of ways during model development. The most critical and easily understood test, however, is whether the calculated sensitivities can be used by the regression to reproduce true parameter values in a synthetic test case. Such an analysis is presented for the synthetic Test Case 1 of the Simulation Examples section.

Compatibility with MODFLOW-2000 Packages

In a single application of MODFLOW-2000, the conductances and storage-related terms of the finite-difference equations are all calculated by a single internal-flow package (Harbaugh and others, 2000, p. 11). While four internal-flow packages have been developed by the U.S. Geological Survey, version 2 of the ADV2 Package is not compatible with the Block-Centered Flow (BCF) (Harbaugh and others, 2000) or the Generalized Finite-Difference (GFD) (Harbaugh, 1992) Packages. The ADV2 Package is compatible with the Layer-Property Flow (LPF) Package (Harbaugh and others, 2000), but it only calculates sensitivities for interblock transmissivities calculated by using the harmonic mean and does not support the alternative calculation schemes. The ADV2 Package also is compatible with the Hydrogeologic-Unit Flow (HUF) Package (Anderman and Hill, 2000), but it only tracks particles through the model layers, rather than through the individual hydrogeologic units, and it calculates sensitivities using the bulk

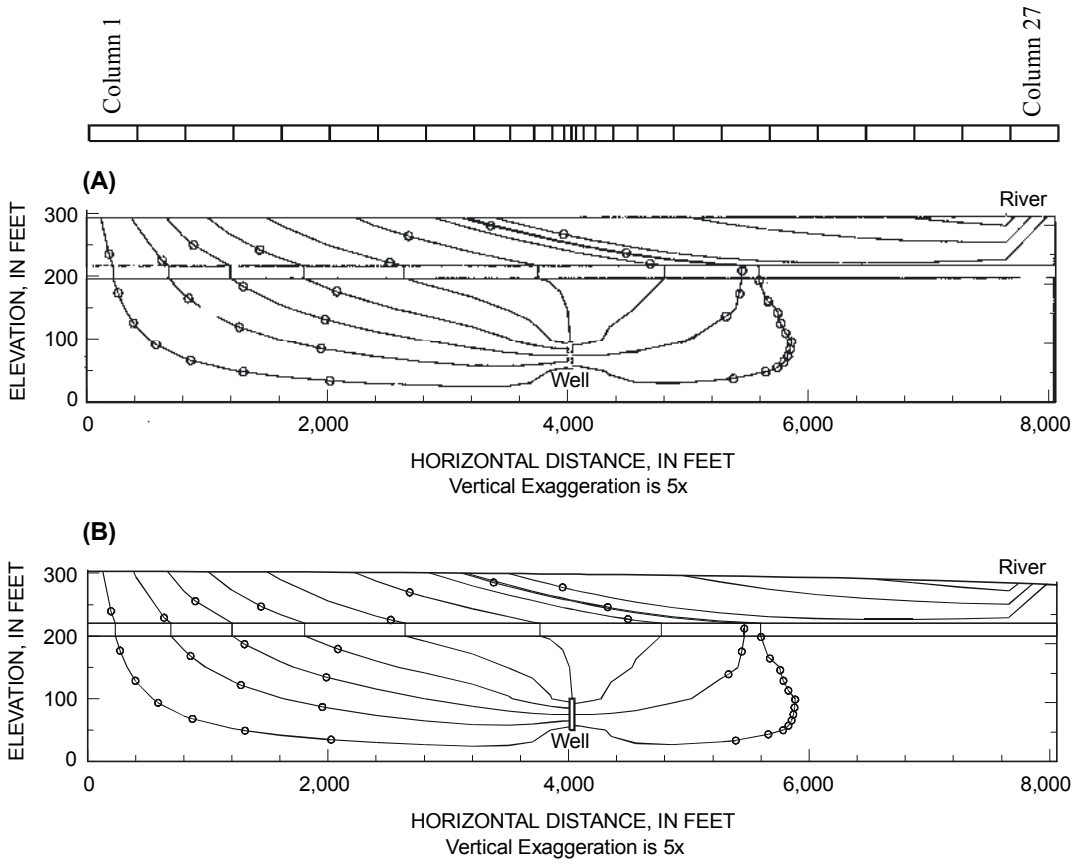

Figure 4. Comparison of MODPATH particle track to ADV2 particle track. (A) Pathlines presented in figure 13 of MODPATH documentation (Pollock, 1989); (B) Pathlines using ADV2 particle-tracking package.

conductances. The ADV2 Package is compatible with the Horizontal Flow Barrier Package (Hsieh and Freckleton, 1993), as adapted for MODFLOW-2000 (see Harbaugh and others, 2000 or "readme" file) for both the LPF and HUF Packages.

The source and sink terms of the finite-difference equations are calculated using stress packages, of which more than one can be used in any given simulation to define boundary conditions. The ADV2 Package uses flows from selected stress packages used to define boundary conditions for the top active layer in the model to calculate vertical particle velocities at cell tops. These are the Recharge (RCH), General-Head Boundary (GHB), Streamflow-Routing (STR), River (RIV), and Drain (DRN) Packages. All other boundary conditions, including other stress packages and constant-head boundaries, applied to the top layer and all boundary conditions applied elsewhere in the model are treated as internal sources of water and are applied at cell centers.

Estimating Effective Porosity

The ADV2 Package does not allow effective porosity to be estimated by the regression. In some situations, this is not expected to be a problem. For example, in Test Case 2 of the section Simulation Examples, the unconsolidated sands have an effective porosity of about 0.39, with little chance of that number being in error by more than 10 percent so that setting the porosity to 0.39 is not expected to cause a problem for parameter estimation. In situations where the possible values of effective porosity span a wide range, porosity will need to be estimated by trial and error when using this package with the Parameter-Estimation Process of MODFLOW-2000. That is, different values of effective porosity can be assumed and the other parameters can be estimated. Alternatively, a more generally applicable parameter-estimation program such as UCODE (Poeter and Hill, 1998) or PEST (Doherty, 1994) can be used to include effective porosity in the regression.

In all circumstances, head and flow observations provide no information on porosity; such information is available only through the advective-transport observations. Also, evaluation of the average linear, or seepage, velocity shows that advective transport is only sensitive to the ratio of hydraulic conductivity and effective porosity. These characteristics suggest that insensitivity and correlation may be problematic when estimating effective porosity.

Obtaining Advective-Transport Observations

For most applications, how to infer advective-transport observations directly from concentration or age data given the complexities contributing to the transport is not clear. Even in the simplest of circumstances, transverse dispersion can cause problems. In addition, in most real-world applications, contaminant release history is poorly known; retardation, decay, and chemical reaction are all taking place to some extent; and few flow fields are truly steady. The purpose of this section is to provide some guidance in the selection of appropriate advective-transport observations based on typically available data.

A simple analysis can provide some insight into the situation and possibly narrow the range of feasible locations of the advective front. For a continuous source in a one-dimensional flow field with homogeneous hydraulic conductivity in the presence of longitudinal dispersion only, the advective front is located along the plume centerline at the 50-percent concentration contour (defined as the concentration halfway between the source concentration and the background concentration). In this situation, longitudinal dispersion causes the contaminant front to spread out along the length of the plume, but the advective front is always located at the farthest point from the source on the 50-percent concentration contour (Domenico and Schwartz, 1990, p. 362). By adding the single complexity of transverse dispersion, the plume front stays closer to the source for a given elapsed time of movement than does the advective front, and the 50-percent concentration contour falls short of the advective front. This problem is illustrated in figure 5, which demonstrates the sensitivity of the location of the 50-percent concentration contour to vertical transverse dispersivity. The presence of transverse dispersion results in the 50-percent concentration contour being located closer to the source than the advective front. The high sensitivity of the location of the 50-percent concentration contour to vertical transverse dispersivity in this problem is due to the small vertical dimension of the contaminant source relative to the horizontal dimension. In general, the location of the 50-percent concentration contour will be more sensitive in situations where transverse dispersion is large in the direction in which the source has a small dimension. For example, the location of the 50-percent concentration contour generated by a tall and narrow source is more sensitive to horizontal transverse dispersion than to vertical transverse dispersion, and the location of the 50-percent concentration contour generated by a short and wide source is more sensitive to vertical transverse dispersion than to horizontal transverse dispersion.

Analytical solutions can aid in the determination of the advective-front location. An example of this approach is given by Anderman and others (1996) and Test Case 2 of Simulation Examples, where the two-dimensional strip-source analytical solution of Wexler (1992) was used to determine the range in normalized concentrations at which the plume advective front might occur for a simulation of the sewage-discharge plume at Otis Air Force Base, Cape Cod, Massachusetts. This range was then used with the contoured concentrations to produce a range of uncertainty in the advective-front location. The source size was varied between 600 and 1,200 ft and the transverse dispersivity was varied between 13 and 30 ft, as indicated by LeBlanc (1984a). Results indicated that the normalized concentration of the plume advective front was between 17 and 43 percent.

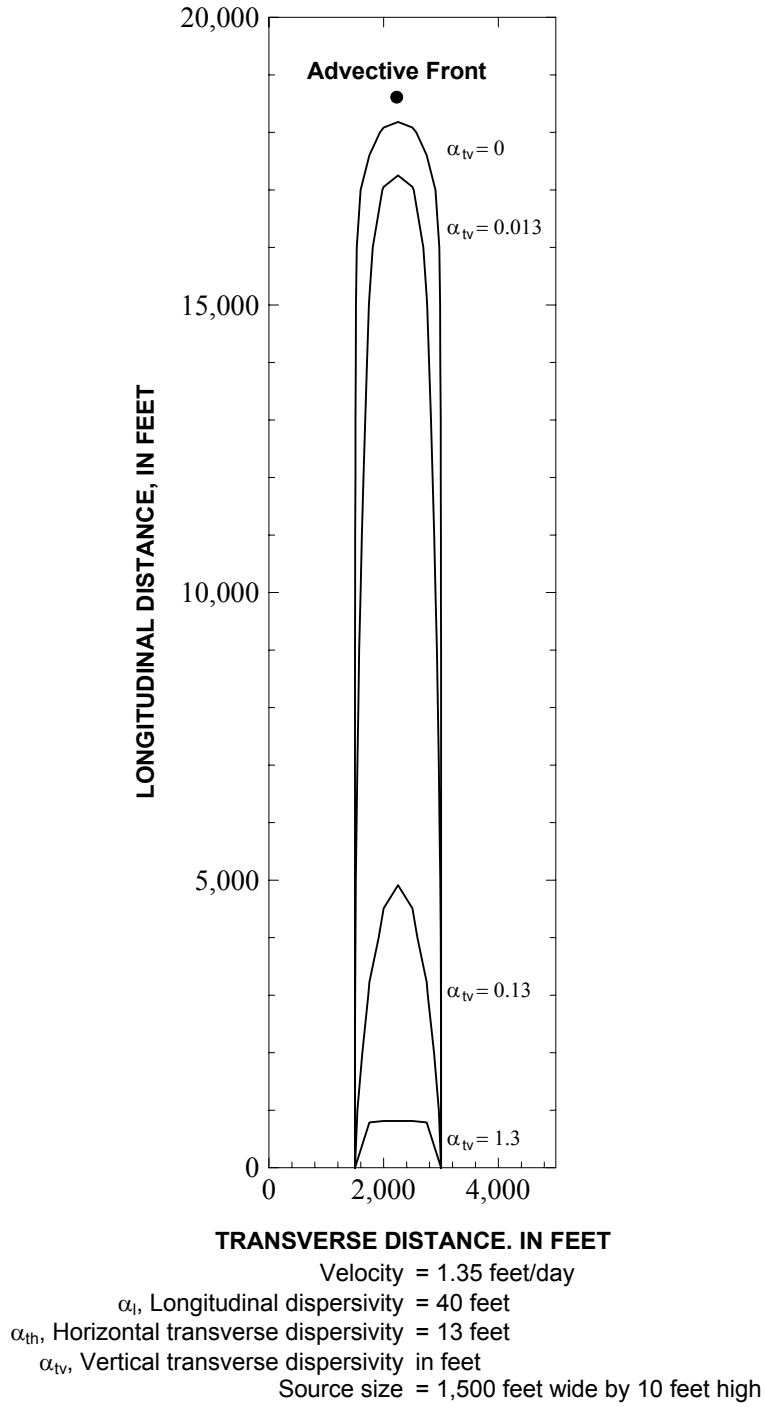

Figure 5. Location of the 50-percent concentration contour with varying vertical transverse dispersivity, calculated using Wexler's (1992) three-dimensional strip source analytical solution.

SIMULATION EXAMPLES

Test Case 1: Example Using Synthetic Data

The validity of the Advective-Transport Observation Package calculations was tested using a problem designed to include features relevant to a typical complex three-dimensional MODFLOW model. A synthetic problem was used so that everything would be known about the system and parameter values; this approach allows analysis not possible with field data. The model grid (fig. 6) has a uniform grid spacing of 1,500 meters(m) in the horizontal and has 247 active cells in each of three layers. Layers 1, 2, and 3 have a constant thickness of 500 m, 750 m, and 1,500 m, respectively. Hydraulic conductivity is divided into four zones, each of which is present in the middle layer and three of which are present in the top and bottom layers (fig. 6). Constant-head boundaries comprise portions of the western and eastern boundaries, with no flow across the remaining boundaries. Head-dependent boundaries representing springs are represented using both the Drain and General-Head Boundary Packages. Wells are present at selected nodes, with pumpage at rates ranging from 100 to 200 m^3/d.

Ten parameters were identified for inclusion in the parameter estimation and are described in table 1 along with their true (assigned) values. The observations used in the parameter estimation were generated by running the model with the true parameter values. The locations of the "observed" hydraulic heads are shown in figure 6. The flows simulated at the head-dependent boundaries (fig. 6) also were used as observations in the parameter estimation. Two advective-transport observations were used in the parameter estimation and were generated by injecting one particle each into two cells along the ground-water high and using the final particle locations after a set period of transport. A homogeneous porosity of 0.3 was used.

When exact observations are used (no noise added), the estimated parameter values duplicate the true parameter values to three significant digits (table 1) in six parameter-estimation iterations, except for the K2, K3, and K4 parameters, which were duplicated to two significant digits. The parameter-estimation closure criterion TOL (Hill and others, 2000, p. 79) was set to 0.01. Thus, parameter estimation using MODFLOW-2000 with the advective-transport package reproduced the true parameter values when exact observations are used in the regression, and this exercise constitutes a validation of the sensitivity and regression calculations.

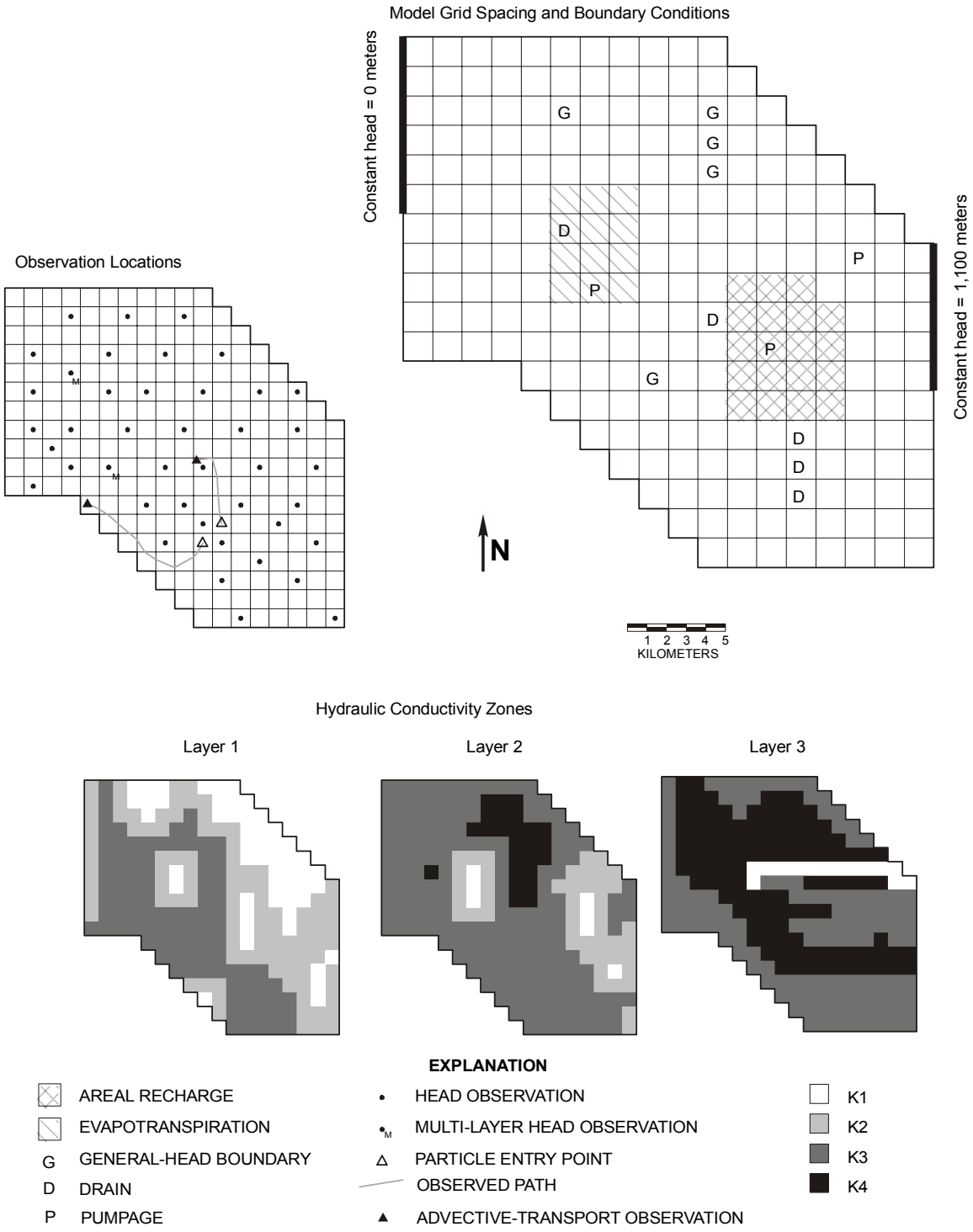

Figure 6. Test Case 1 model grid, boundary conditions, observation locations, and hydraulic conductivity zonation used in parameter estimation.

Table 1. Labels, descriptions and estimated values for the parameters for Test Case 1
[m/d, meter per day; m^2/d, square meters per day]

Label	Description	Units	True Value	Estimated Value
K1	Hydraulic conductivity of zone 1 (fig. 6)	m/d	1.00	1.00
K2	Hydraulic conductivity of zone 2 (fig. 6)	m/d	$1.00x10^{-2}$	$0.99x10^{-2}$
K3	Hydraulic conductivity of zone 3 (fig. 6)	m/d	$1.00x10^{-4}$	$0.99x10^{-4}$
K4	Hydraulic conductivity of zone 4 (fig. 6)	m/d	$1.00x10^{-6}$	$0.99x10^{-6}$
ANIV1	Vertical anisotropy of layers 1 and 2		4.00	4.00
ANIV2	Vertical anisotropy of layer 3		1.00	1.00
RCH	Areal recharge rate (fig. 6)	m/d	$3.10x10^{-4}$	$3.10x10^{-4}$
ETM	Maximum evapotranspiration rate (fig. 6)	m/d	$4.00x10^{-4}$	$4.00x10^{-4}$
GHB	Conductance of head-dependent boundaries G (fig. 6) represented using the General-Head Boundary Package.	m^2/d	1.00	1.00
KDR	Conductance of the head-dependent boundaries D (fig. 6) using the Drain Package.	m^2/d	1.00	1.00

Test Case 2: Example Using Field Data

The ADV2 Package was applied to the sewage-discharge plume at Otis Air Force Base on the Massachusetts Military Reservation in Cape Cod, Massachusetts (fig. 7) to demonstrate, using a previously published field-site simulation, the use of advective-transport observations in model calibration with parameter estimation accomplished using nonlinear regression. The site was chosen because field studies had been conducted to characterize the plume and the hydrogeological setting of the area and because a two-dimensional ground-water flow model had been developed by using trial-and-error calibration by LeBlanc (1984a). This test case is presented by Anderman and others (1996) but is repeated here to provide insight into the use of advective-transport observations in ground-water-flow model calibration. In addition, the test case illustrates some useful procedures that are applicable regardless of the types of observations considered.

Site Description

The regional aquifer is part of an outwash plain and consists of an approximately 330-ft thick unit of unconsolidated sediment overlying relatively impermeable bedrock (LeBlanc and others, 1991). The aquifer consists of 100 ft of unconsolidated sand and gravel sediments and is underlain by a confining unit consisting of approximately 230 ft of fine-grained sand and silt. Regional estimates of hydraulic conductivity of the aquifer based on grain-size distributions, ground-water flow model calibration, and one aquifer test range from 140 to 370 feet per day (ft/d) (LeBlanc, 1984a; LeBlanc and others, 1991). Flow-meter analyses on 16 long-screened wells in a gravel pit adjacent to Ashumet Pond yielded an average hydraulic conductivity of 310 ft/d (Hess and others, 1992). The effective porosity of the outwash determined from spatial

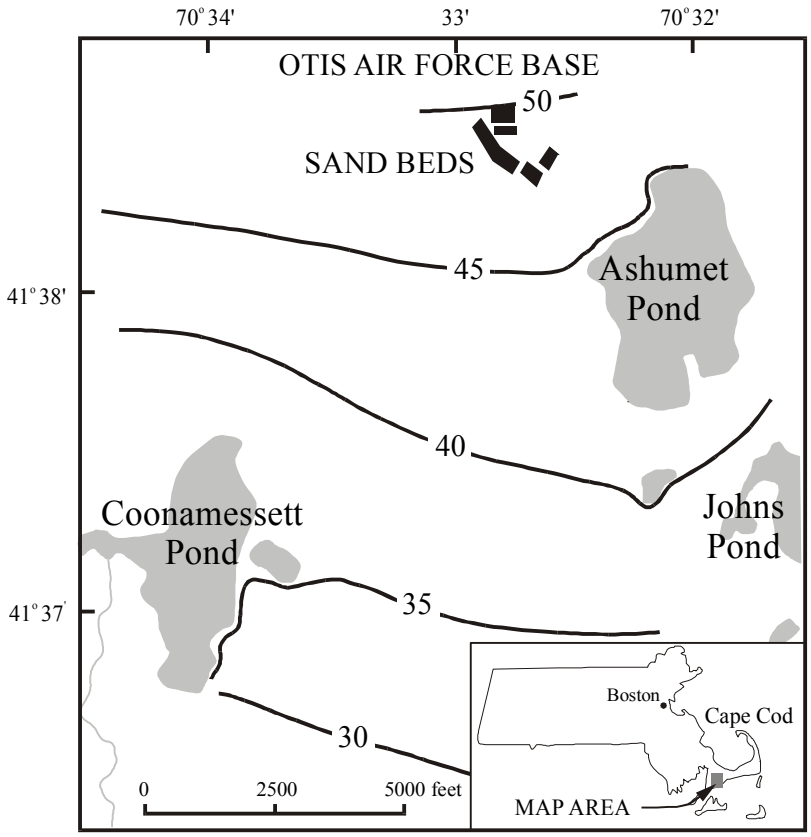

Figure 7. Location of Otis Air Force Base, water-table elevation contours, and sewage-discharge sand beds for Test Case 2 (modified from LeBlanc, 1984b).

moments analysis of several small-scale tracer tests is about 0.39. Vertical hydraulic-head gradients within the aquifer are small, and ground-water flow in the aquifer can be considered to be horizontal, with an average regional flow to the south-southwest (LeBlanc and others, 1991).

The plume emanates from sand beds (fig. 7) used for sewage disposal since the 1930's, although appreciable discharge to the beds did not commence until the early 1940's. A number of physical properties and chemical constituents have been monitored to determine the extent and migration of the sewage plume. Boron, contoured by LeBlanc (1984a) during 1978-79 measurements (fig. 8), is a good indicator of plume movement because of its high concentration relative to uncontaminated ground water. Data indicate that boron transport is slightly retarded (Warren Wood, U.S. Geological Survey, written commun., 1994), but analysis of the retardation rates indicated that the effect on inferred rates of advective transport is negligible.

Ground-Water Flow and Parameter-Estimation Models

The movement of contaminants in the sewage-discharge plume was simulated using a two-dimensional finite-difference ground-water flow model based on the model developed by LeBlanc (1984a) (fig. 8A). The model has thirty-four 500-ft wide columns and thirty-eight 750-ft long rows, with 957 active cells. LeBlanc (1984a) used a homogeneous hydraulic conductivity of 186 ft/d; recharge to the aquifer from precipitation of 19.8 inches per year(in/yr), with no recharge over Ashumet Pond; specified flux across the northern boundary at about the 60-ft water-table contour of 2.3 cubic feet per second (ft^3/s); constant head along (1) the southern boundary at about the 10-ft water-table contour, (2) Coonamessett Pond and River on the west side of the model, and (3) Johns Pond and the Childs River on the east side. Ashumet Pond was represented as a general-head boundary, with two zones of conductance: the outer shoreline zone had 10 times the hydraulic conductivity and one-fifth the thickness of the inner zone. The decrease in aquifer thickness beneath the pond was simulated by tapering the saturated thickness of the layer beneath the pond to one-half of the saturated thickness of the aquifer. Two head-dependent river reaches were simulated within the model area: Cranberry Bogs near the southern boundary of the model, and the area north of Johns Pond on the eastern boundary of the model. The sewage-discharge sand beds were represented as a specified-flux boundary with a flux of 0.72 ft^3/s, which is based on estimates of historical discharge. The boundaries north of Coonamessett and Johns Ponds correspond to ground-water flow lines and are simulated as no-flow boundaries.

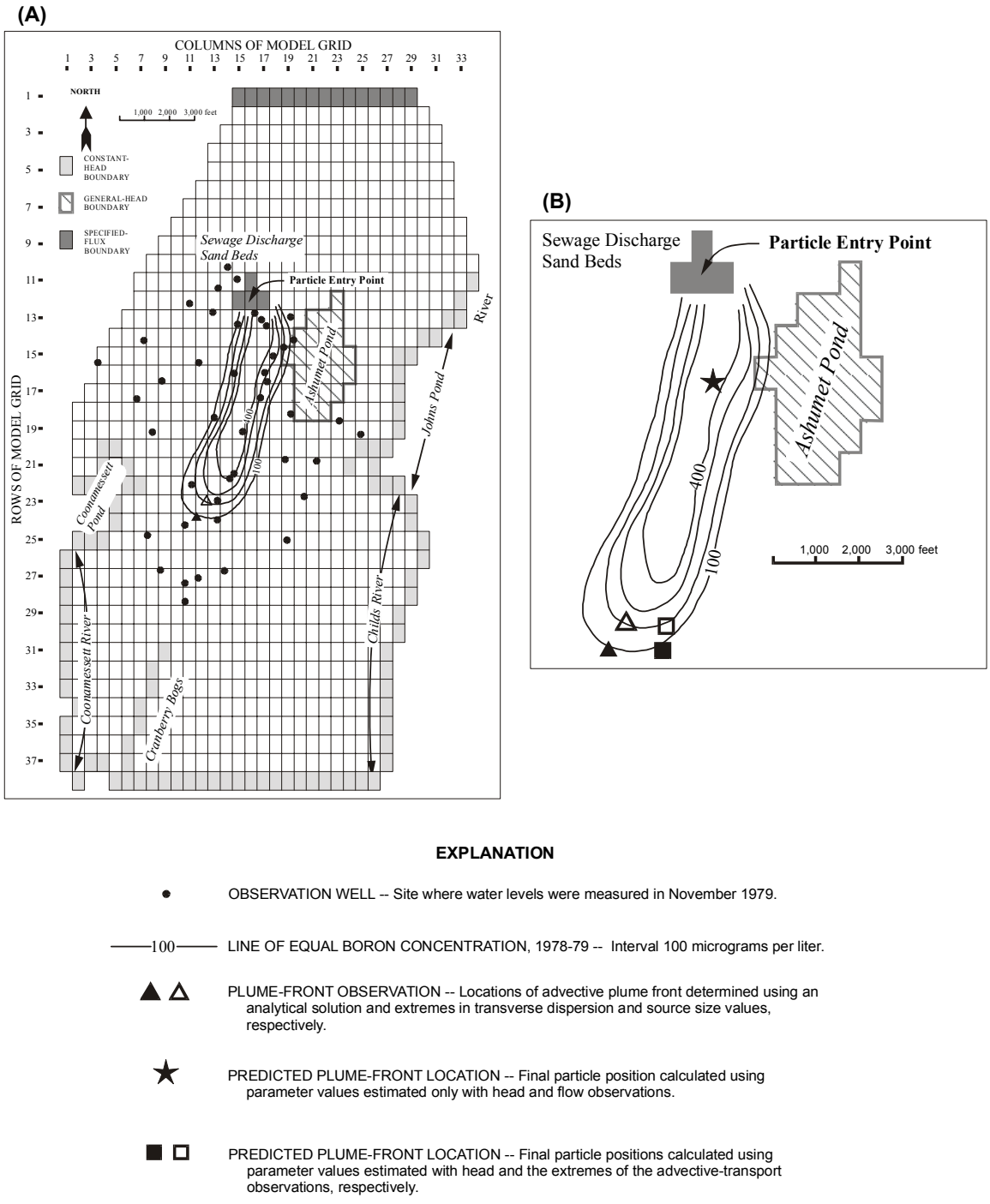

EXPLANATION

- OBSERVATION WELL -- Site where water levels were measured in November 1979.
- 100 — LINE OF EQUAL BORON CONCENTRATION, 1978-79 -- Interval 100 micrograms per liter.
- ▲ △ PLUME-FRONT OBSERVATION -- Locations of advective plume front determined using an analytical solution and extremes in transverse dispersion and source size values, respectively.
- ★ PREDICTED PLUME-FRONT LOCATION -- Final particle position calculated using parameter values estimated only with head and flow observations.
- ■ □ PREDICTED PLUME-FRONT LOCATION -- Final particle positions calculated using parameter values estimated with head and the extremes of the advective-transport observations, respectively.

Figure 8. (A) Test Case 2 finite-difference grid, observation wells, boron concentrations of contaminated ground water, and advective-transport observation locations used in the regression (modified from LeBlanc, 1984a); (B) Detail of the sewage-discharge plume and advective-front locations calculated using the sets of estimated parameter values shown in tables 3B, 3C, and 3E.

Five parameters were identified for estimation by the parameter-estimation model: (1) the homogeneous hydraulic conductivity (K), (2) areal recharge (RCH), (3) flux at the northern boundary (Qn), (4) flux at the sewage-discharge beds (Qb), and (5) the conductance of the low hydraulic conductivity zone of Ashumet Pond (GHB) (the conductance of the outer zone equals this parameter value times 50). The inclusion of specified-flux boundary conditions as parameters allowed their values to vary with changes in the hydraulic-conductivity parameter, as would be expected. Inclusion of a sixth parameter representing the conductance of Coonamessett and Childs Rivers caused unstable regression results due to this parameter's insensitivity; thus, the rivers are represented using constant-head cells for the results presented. The ground-water flow model developed for the present work duplicates that described by LeBlanc (1984a) when his parameter values are used.

Observations used in the parameter estimation included (1) 44 measured hydraulic heads, which are considered to be accurate; (2) a head-dependent boundary recharge of 0.4 ft^3/s from Ashumet Pond determined from a water budget, which is considered to be somewhat unreliable; and (3) observed x- and y-locations of the advective front estimated from the boron concentration contours, which are considered to be somewhat reliable. The locations of Ashumet Pond, the observation wells, and the advective-transport observations are shown in figure 8A. The triangles in figure 8 represent the extreme advective-front locations estimated based on the analysis procedure described in the section Obtaining Advective-Transport Observations. Use of the two advective-transport observations allowed for investigation of how uncertainty in advective-front observations affect parameter-estimation model results. To simulate the advective transport, a single particle was introduced into the ground-water system at the approximate center of the plume source in the middle of the cell in row 12, column 16 (fig. 8A), and was allowed to move for the 38-year period between appreciable discharge to the aquifer and the time of observation.

The weights of these observations were calculated using the following statistics, as discussed after equation 1: The standard deviation of the 44 accurate hydraulic-head measurement errors was assumed to be 0.1 ft; the coefficient of variation (standard deviation divided by the measured value) of the somewhat unreliable head-dependent boundary measurement error was assumed to be 0.5; the standard deviation of each of the somewhat reliable advective-front movement observations was assumed to be 500 ft (the width of a grid cell) in both the x- and y-directions.

Analysis Procedure

To quantify the effect of observation type, the parameter-estimation model was run with six different sets of observations: (1) head observations alone, (2) head and flow observations, (3, 4) head and each of the two advective-transport observations, and (5, 6) head, flow, and each of the two advective-transport observations.

Each data set was evaluated in two ways, which are presented here because of their utility in inverse modeling. First, in a preliminary analysis, initial parameter value regression statistics, including the overall parameter sensitivities and correlations, were calculated at the parameter values reported by LeBlanc (1984a). Correlations are obtained at initial parameter values by setting MAX-ITER in the Parameter-Estimation (PES) Process input file to zero (Hill and others, 2000, p. 79). Results from the preliminary analysis can be used to identify parameter insensitivity and correlation that is likely to cause problems in the nonlinear regression and to evaluate the likely effect of any new or proposed observation on parameter sensitivity and correlation. This information can then help guide redefinition of the parameters, if necessary. Because the ground-water flow equation is nonlinear with respect to many estimated parameters, the results for the initial parameter values may differ from the results calculated at other sets of parameter values, but the major characteristics are often similar. In a second set of model runs, parameter values are optimized using nonlinear regression, and their overall sensitivities, correlations, and coefficients of variation are calculated. The statistics used in the analysis are discussed more fully in the following paragraphs.

The overall sensitivity of the simulated observation equivalents to the parameters reflect how well the parameters are defined by the observations and indicate how well the parameters will be estimated. Composite scaled sensitivities are used to measure this overall sensitivity and are calculated by MODFLOW-2000 as follows. First, the sensitivities are scaled by multiplying them by the product of the parameter value and the square root of the weight of the observation to obtain dimensionless values. The scaled sensitivities for each parameter are then squared and the sum of these values is divided by the number of observations. The composite scaled sensitivities equal the square root of these values and are listed in the MODFLOW-2000 output. The scaling depends on the parameter values, and, for nonlinear parameter-estimation models, the sensitivities depend on the parameter values. Consequently, the composite scaled sensitivities will be different for different parameter values. As mentioned above, however, the major characteristics are often similar. The authors' experience indicates that if the composite scaled sensitivity values for each

of the parameters vary from each other by more than two orders of magnitude, the optimization procedure often has difficulty estimating values for the less sensitive parameters.

As previously discussed, correlation between parameters indicates whether or not the parameter estimates are unique with the given model construction and observations, depending on how well the parameters are defined by the observations. Correlations range between -1 and 1, with absolute values close to 1 indicating a high degree of correlation. If two parameters are highly correlated, then changing the parameter values in a linearly coordinated way will result in a similar value of the objective function. Parameter correlation is a concern in trial-and-error calibration as well, but may be unknown to the modeler; the use of regression makes parameter correlation obvious. Although there is debate over what correlation values are significant, the authors' experience has indicated that there is enough information in the observation data so that parameters can be uniquely estimated if their correlation is less than 0.98. For correlations with absolute values larger than 0.98, uniqueness of the solution can be evaluated by starting parameter estimation at different initial values. If all runs produce nearly the same estimates, the solution is probably unique.

The coefficients of variation of the estimated parameter values are calculated as the standard deviations of the parameter estimates divided by the estimated parameter values. Values much less than 1.0 occur when the parameter has a large overall sensitivity and indicate a precise parameter estimate.

Results

At the LeBlanc parameter values (table 2), composite scaled sensitivities are not significantly affected by either the flow or transport observations, but the flow observation (table 2B) reduces the correlations more than does the advective-transport observation (table 2C). The complete parameter correlations produced when head observations (table 2A) are used alone indicates that estimating parameters independently with head observations alone will be impossible. Adding flow or advective-transport observations reduced some of the correlations, but the remaining correlations of 1.0 and the low sensitivity for the Ashumet Pond (GHB) conductance still indicate possible problems. These results suggest that, as weighted, (1) the flow observation is more valuable to the regression than is the advective-transport observations, (2) both additional observations can help to reduce the extreme correlation that occurs when only

Table 2. Parameter sensitivities and correlations calculated for the initial parameter values for Test Case 2

[The labels K, RCH, Qn, Qb, and GHB are used to identify the following estimated parameters: K, hydraulic conductivity; RCH, recharge rate; Qn, northern boundary flux; Qb, sewage-discharge sand bed flux; GHB, Ashumet Pond conductance.]

	K	RCH	Qn	Qb	GHB
LeBlanc's Values	186	19.8	2.3	0.72	64,800
	A. Head observations only				
Composite sensitivity	39.0	29.9	6.57	3.88	0.0572
	Correlation calculated at initial values				
RCH	1.00				
Qn	1.00	1.00			
Qb	1.00	1.00	1.00		
GHB	1.00	1.00	1.00	1.00	
	B. Head and flow observations				
Composite sensitivity	39.0	29.8	6.57	3.86	0.0568
	Correlation calculated at initial values				
RCH	1.00				
Qn	0.93	0.92			
Qb	0.72	0.71	0.43		
GHB	0.01	0.00	-0.01	0.26	
	C. Head and near advective-transport observations				
Composite sensitivity	38.2	29.2	6.43	3.80	0.0571
	Correlation calculated at initial values				
RCH	1.00				
Qn	1.00	1.00			
Qb	1.00	1.00	1.00		
GHB	0.75	0.75	0.75	0.76	

hydraulic-head observations are used to estimate parameter values, and (3) problems with the regression are likely. Further investigation showed that at the initial parameter values the advective-transport observation does not significantly reduce the correlations because the particle only travels a short distance and discharges into Ashumet Pond. This may indicate that, in this case, the analysis procedure is limited because the starting parameter values produce unreasonable advective transport. It also indicates the importance of investigating the model fit associated with the initial parameter values.

The model fits achieved in the regression presented in table 3 are summarized as follows. Table 3A shows that regression was not possible using head data alone. The addition of the flow observation reduced the correlation so that the regression converged, which is consistent with the preliminary analysis, but the optimal parameter values shown in table 3B are unreasonably small. At the optimal parameter values produced by using the advective-transport observations (tables 3C and 3E), the parameters are less correlated than at the optimal parameter values produced using the flow observation (table 3B), which is inconsistent with the preliminary analysis above. Inspection of the results indicated that this inconsistency was caused by the fact that, with LeBlanc's values, the particle exited into Ashumet Pond, as noted above. The smaller coefficients of variation produced using the advective-transport observations indicate the estimates are more precise than those produced using the flow observation. Using all the observations (tables 3D and 3F) results in parameter estimates, correlations, and coefficients of variation that are very close to those using the head and advective-transport observations. The small composite scaled sensitivity and large coefficient of variation for the northern boundary flux and Ashumet Pond conductance indicate that these parameters are not well defined with the available observations and given model construction.

When parameter values were optimized using nonlinear regression, the total objective function (S of eq. 1) was reduced from about 4,500 to about 1,700 for all simulations. This results in a calculated error variance of 39, suggesting that the model fit to the data is worse than would be consistent with the subjectively determined standard deviations and coefficient of variation by, on average, a factor of the square root of 39, or about 6. This difference could be due to neglecting some components of the measurement error or to model error (Hill, 1998).

Table 3. Optimal parameter estimates, parameter sensitivities, and correlations for Test Case 2

[The labels K, RCH, Qn, Qb, and GHB are used to identify the following estimated parameters: K, hydraulic conductivity; RCH, recharge rate; Qn, northern boundary flux; Qb, sewage-discharge sand bed flux; GHB, Ashumet Pond conductance. Values in parentheses are the total number of parameter-estimation iterations required to satisfy a convergence criteria of 0.01; * indicates convergence was not achieved in 15 iterations, estimates from the final iteration are reported; - -, not calculated because parameter estimation did not converge.]

	K	RCH	Qn	Qb	GHB
LeBlanc's / Initial Values	186	19.8	2.3	0.72	64,800

	A. Head observations only (*)					B. Head and flow observations (8)				
	K	RCH	Qn	Qb	GHB	K	RCH	Qn	Qb	GHB
Estimated value	209	14.5	4.1	0.80	1,490	46	3.2	0.9	0.18	328
Composite sensitivity	35.2	21.2	11.5	4.21	1.25	34.9	21.0	11.4	4.19	1.22
Coefficient of variation	- -	- -	- -	- -	- -	3.4	3.4	3.5	3.6	3.6
	Correlation calculated at optimal values					Correlation calculated at optimal values				
RCH	1.0					1.00				
Qn	1.0	1.0				0.99	0.99			
Qb	1.0	1.0	1.0			0.94	0.94	0.89		
GHB	1.0	1.0	1.0	1.0		0.96	0.95	0.95	0.92	

With Near Boron Plume Observation

	C. Head and advective-transport observations (6)					D. All observations (6)				
	K	RCH	Qn	Qb	GHB	K	RCH	Qn	Qb	GHB
Estimated value	158	10.9	3.1	0.60	1,122	147	10.2	3.0	0.49	955
Composite sensitivity	34.5	20.7	11.4	4.06	1.22	34.5	20.7	11.7	3.58	1.27
Coefficient of variation	0.3	0.3	0.6	1.3	1.1	0.3	0.4	0.6	1.4	1.0
	Correlation calculated at optimal values					Correlation calculated at optimal values				
RCH	0.95					0.96				
Qn	0.63	0.55				0.68	0.60			
Qb	0.14	0.08	-0.59			0.07	0.02	-0.60		
GHB	0.31	0.17	0.24	0.26		0.31	0.17	0.27	0.23	

With Distant Boron Plume Observation

	E. Head and advective-transport observations (6)					F. All observations (6)				
	K	RCH	Qn	Qb	GHB	K	RCH	Qn	Qb	GHB
Estimated value	169	11.7	3.3	0.63	1,200	158	11.0	3.2	0.51	1,009
Composite sensitivity	34.5	20.7	11.4	4.04	1.20	34.7	20.8	11.9	3.48	1.29
Coefficient of variation	0.3	0.3	0.6	1.3	1.1	0.3	0.3	0.6	1.4	1.0
	Correlation calculated at optimal values					Correlation calculated at optimal values				
RCH	0.94					0.95				
Qn	0.60	0.50				0.66	0.56			
Qb	0.10	0.03	-0.65			0.04	-0.02	-0.64		
GHB	0.28	0.12	0.21	0.25		0.28	0.13	0.25	0.21	

Starting at the LeBlanc values, the reduction of the objective function for all regression runs were similar, as follows: for hydraulic heads, S_h decreased from about 4,150 to about 1,675, and unweighted hydraulic-head residuals exceeded 1.0 ft at five observation points and did not exceed 1.5 ft (3 percent of the total 50-ft head drop across the system and substantially larger than the 0.1-ft standard deviation used to weight the head observations); for the flow out of Ashumet Pond, S_f increased from 5 to about 20, and the unweighted residual did not exceed 0.86 ft^3/s (215 percent of the observed flow or about four times the coefficient of variation used to weight the flow observation); for the near advective-transport observation, S_t decreased from 173 to less than 5, and the x- and y-residuals did not exceed 1,050 and 560 ft, respectively (roughly double and equal to the standard deviations, respectively, used to weight the advective-transport observations); for the distant advective-transport observation, S_t decreased from 218 to less than 10, and the x- and y-residuals did not exceed 1,360 and 565 ft, respectively (roughly two and a half times and equal to the standard deviations, respectively, used to weight the advective-transport observations).

These results indicate that the lack of model fit that resulted in the error variance of 39 was spread throughout the observations, and that no one type of observations was fit better overall than another, as is required for a valid regression. Analysis not included in this report indicates that the weighted residuals are independent and normally distributed. There is an area of the model west of Ashumet Pond and north of Coonamessett Pond, however, where the calculated heads are consistently higher than the observed heads, indicating some bias in the model. The source of this bias was not determined in this study.

The parameter values estimated when the distant advective-transport observation is used (tables 3E and 3F) are an average of 7 percent higher than those estimated when the near observation is used (tables 3C and 3D). This can be explained by the difference in the observed locations (fig. 8): the distant observation implies that the advective front is moving with an average velocity of 0.65 ft/d, 8 percent faster than the average velocity of 0.60 ft/d implied by the near observation. For the two sets of parameter estimates, the ninety-five percent linear individual confidence intervals calculated largely overlap, indicating that the estimated values are not statistically different. Thus, for this model, even though the location of the advective front is not well known, the parameter estimates do not change significantly when considering reasonable uncertainty in the advective-transport observation.

Discussion

Advective-transport observations reflect ground-water velocities and patterns over a long period of time and provide more complete information about the ground-water flow system than do flow measurements taken at a discrete point in time. This results in different estimated parameter values when different observation types are used (tables 3B, 3C, and 3E) and has a significant effect on the probable accuracy of the transport predictions of the model. Figure 8B shows that the advective-front location simulated using the parameter values estimated with only the head and flow observations (represented by the star) is at least 6,085 feet from the plume-front observation locations (represented by the open and closed triangles), while the locations simulated using the parameter values estimated with only the head and advective-transport observations (represented by the open and closed squares) are at most 1,275 feet from the plume-front observation locations. This illustrates that the use of advective-transport observations in the parameter estimation results in a model that more accurately represents the movement of the sewage-discharge plume than use of the flow observation. Results not presented in this report also show that the particle-position sensitivities and flow sensitivities are of opposite sign, which means that the particle-position and flow observations cause the parameter values to change in opposite directions.

In simulations in which only one observation reduces correlation in an otherwise completely correlated set of parameters, the simulated equivalent to that observation is always very close to the observed value. In Test Case 2, this occurs in simulations with only the flow observation or only the advective-transport observations. In this circumstance, the close match does not necessarily indicate an accurate simulation, but is an artifact of the relation between the data and the parameter values, and any error in that observation is directly translated into the solution. In many cases confidence intervals will be large, reflecting the underlying uncertainty.

Ground-water flow model validity can be judged by evaluation of the reasonableness of the parameter estimates and the lack of bias in the weighted residuals (Draper and Smith, 1981; Cooley and Naff, 1990). For all simulations using the advective-transport observations (tables 3C through 3F), the estimated values of horizontal hydraulic conductivity (K) are within the reported range of 140 to 370 ft/d and, with a coefficient of variation of about 0.3 (table 3), can be considered to be precisely estimated with the available data. The estimated northern boundary flux (Qn) is roughly 1.3 to 1.4 times the flux used by LeBlanc (1984a), which is not unreasonable considering how little is known about this flux. The estimated sewage discharge flux (Qb) is as little as two-thirds of LeBlanc's value, which may be a little low, but is reasonable considering

precise estimation was not possible with the available data, as indicated by the somewhat large coefficient of variation of 1.0 to 1.1.

The estimated Ashumet Pond conductance (GHB) and recharge (RCH) parameter values for the simulation using all observations (tables 3D and 3F) are about a factor of 64 and 2, respectively, less than the values used by LeBlanc (1984a). Evaluating whether the estimated Ashumet Pond conductance parameter value is reasonable given the lack of field data is difficult. Considerable independent information, however, indicates that the recharge rate should be close to 20 in/yr (LeBlanc, 1984a), so the estimated 11-in/yr recharge rate appears to be unreasonably small. Possible explanations developed as part of this study include: (1) the heads used in the model were measured in November and may not represent average annual conditions, and (2) the elevations of the constant-head boundaries were determined from 10-ft contour topographic maps, and, therefore, are subject to errors of 5 ft or more. The seasonal variation in the water-table elevation is 1 to 3 feet, with the lowest heads occurring in late fall (LeBlanc, 1984b). The importance of the observation-well and boundary-head elevations to the model was investigated by estimating parameter values with all the observations with the distant advective-transport observation and (1) all the observed-head elevations increased by 1 ft, or (2) all the constant-head elevations decreased by 1 ft. Increasing all the observed head elevations resulted in an estimated recharge rate of 22.1 in/yr, while decreasing the constant-head elevations resulted in an estimated recharge rate of 15.2 in/yr. These results suggest that model results are sensitive to the relation between the observed heads and the constant-head boundary heads, and, therefore, that it is important to either measure all head elevations used in the model at the same time, or to measure the head elevations at multiple times and to use an average in the model. These results also demonstrate how nonlinear regression can be used to test different aspects of model calibration.

FIRST-ORDER UNCERTAINTY ANALYSIS

Output from the ADV2 package is compatible with the three post-processors for testing residuals and calculating linear confidence and prediction intervals from MODFLOW-2000 results (Hill and others, 2000). Directions for producing the files in MODFLOW-2000 necessary to run the post processors are given by Hill and others (2000, p. 85).

The confidence intervals calculated by post-processor YCINT-2000 (Hill and others, 2000, p. 87) for calibrated or predicted conditions can be used to construct confidence interval regions for the predicted advective-transport observations. Output from YCINT-2000 consists of 95-percent confidence intervals along the x-, y-, and z-coordinate directions. It can be useful to simply plot these confidence intervals on their respective axes, as shown in a plot of the x-y plane for Test Case 1 (fig. 9A).

To better display the confidence intervals, the confidence intervals also can be used to construct an ellipse in two dimensions or an ellipsoid in three dimensions. An ellipsoid can be constructed using output from either the #yc or _yp file generated by YCINT-2000, which consists of 95-percent confidence or prediction intervals along the x-, y-, and z-coordinate directions. The resulting ellipsoid does not generally constitute a confidence region because of model nonlinearity and because the direction of the major grid axes of the confidence region are not known. The ellipsoids can be used, however, to clearly display the confidence intervals if suitable axis directions can be defined.

One alternative is to require that one of the axes be aligned with the direction of flow. Then, the intervals along the x-, y-, and z-coordinate directions can be used to define points on the surface of the ellipsoid, and the entire ellipsoid can be constructed using these points. An example of an ellipse constructed in this way using confidence intervals calculated using the ADV2 Package is shown in figure 9B.

The confidence intervals shown in figure 9 are smaller than would be encountered for most models because noiseless observations were used in the parameter estimation, and, therefore, the graphs of figures 9A and B are exaggerated roughly by a factor of 2,200. For both calculated particle locations, the confidence interval parallel to the flow direction is much smaller than the interval perpendicular to the flow direction. This is consistent with larger dimensionless scaled sensitivities in the y-direction relative to the x-direction.

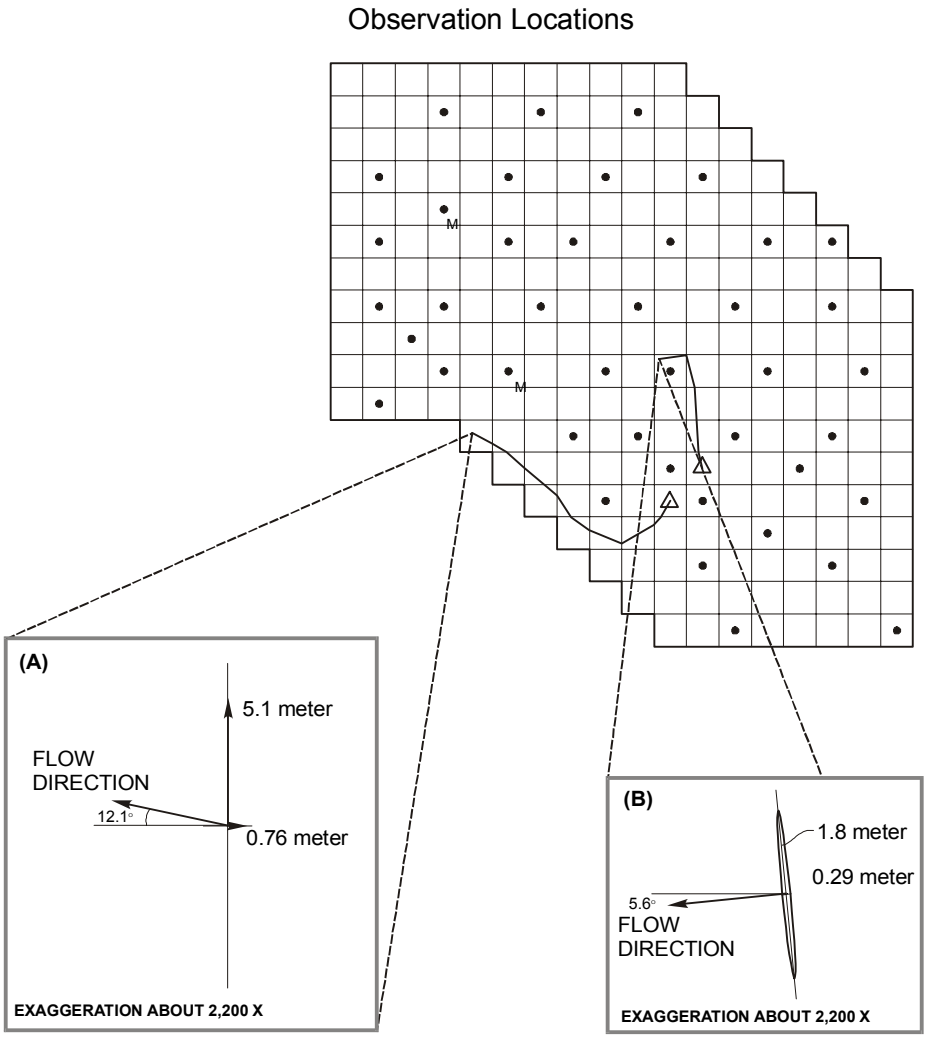

Figure 9. 95-percent individual confidence intervals for final calibrated advective-transport observations for Test Case 1. (A) The intervals are plotted in their respective coordinate axis directions; (B) The intervals are used to plot an ellipse oriented such that the primary axes are oriented parallel and perpendicular to the flow direction at this location.

COMMON PROBLEMS

A number of problems are commonly encountered when using advective-transport observations in regression. Some of the most common problems are discussed here. The use of advective-transport observations may not be appropriate for all situations.

1. Problem: The particle track at the starting parameter values is very different than the observed track.

   Discussion: Commonly a particle will track in a very different direction than observed using the starting parameter values and perhaps exit the model grid prematurely. For example, the particle track at the starting parameter values for the Otis Air Force Base model of Test Case 2 exits into Ashumet Pond (fig. 10). This results in large advective-transport residuals and smaller than expected sensitivities that are not reflective of the true worth of the data.

   Resolution: Often this problem resolves itself. As the parameter values are changed by the regression during the parameter-estimation iterations so that they are more reflective of the actual system, the simulated particle track generally will also start looking more like the observed track. For example, the final particle position for Test Case 2 is very close to the observed plume-front location (fig. 8B). If it does not resolve itself and the final track is incorrect, see Problem 2.

2. Problem: The particle track at converged parameter values is much different than the observed track.

   Discussion: Possible causes include (a) the entry point of the particle into the system is incorrect, (b) one of the other observations or prior information may be dominating the regression, and (c) there are errors in the conceptual representation of the system.

   Resolution: For (a), it is important that the point where the particle is introduced into the model grid be chosen with care. If the entry point is located on a high point in the water table from which flow diverges, then the high point may move around with differing parameter values and the resulting particle track can be very erratic. Likewise, if the entry point is close to a dominant ground-water sink, the particle may track towards the sink and exit the system prematurely.

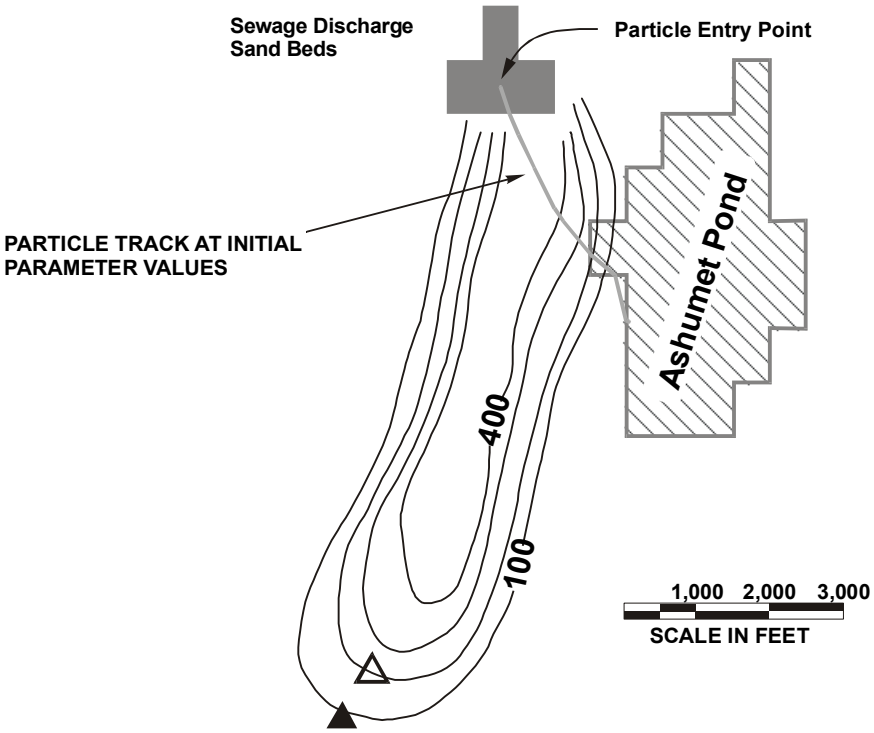

Figure 10. Example of unrealistic particle track at starting parameter values for Test Case 2.

Changing the entry point even slightly may result in a more realistic particle track; a few trial runs may be needed to obtain an entry point that seems appropriate. If a problem is very sensitive to different, but equally likely, initial particle placements, this should be discussed in any description of the calibration effort. For (b), the data from which the observations and their weights were calculated need to be carefully scrutinized. Observations that have large weighted residuals and scaled sensitivities will dominate the regression and should be examined first. Specifically, look at how the water-table elevations were determined, and whether well-head elevations were surveyed precisely or taken from a topographic map. Alternatively, if the model grid-cell spacing is large and the water table has a steep gradient, model error may be a larger factor than anticipated. An observation that is causing a problem may be less precise than initially indicated, so that the statistic from which the weight is calculated should be increased, or it may be inaccurate, so that it should be omitted from the parameter estimation. For (c), any of the assumptions on which the conceptual model is based may be in error. Commonly, aquifer heterogeneity is oversimplified or incorrectly specified, or specified boundary conditions are in error. Again, scrutinize the model setup and revise model input.

3. Problem: Complex particle tracks may cause the regression not to converge.

Discussion: An example of this problem occurred for Test Case 1 (fig. 11). Here, the particle is introduced into the system at the water table (layer 1) in row 12 and column 13, travels to layer 2, back up to layer 1, descends to layer 3, traverses the model, and finally emerges from layer 1 with evapotranspiration in row 7 and column 7. This circuitous path follows patches of high hydraulic conductivity. When the coordinates of the endpoint of this path are included as observations, the parameter estimation oscillates and does not converge, even when exact observations are used. The parameter estimation converges normally if this observation is omitted.

Resolution: If intermediate or additional advective-transport data are available, use these in the parameter estimation as well. Otherwise, omit the advective-transport

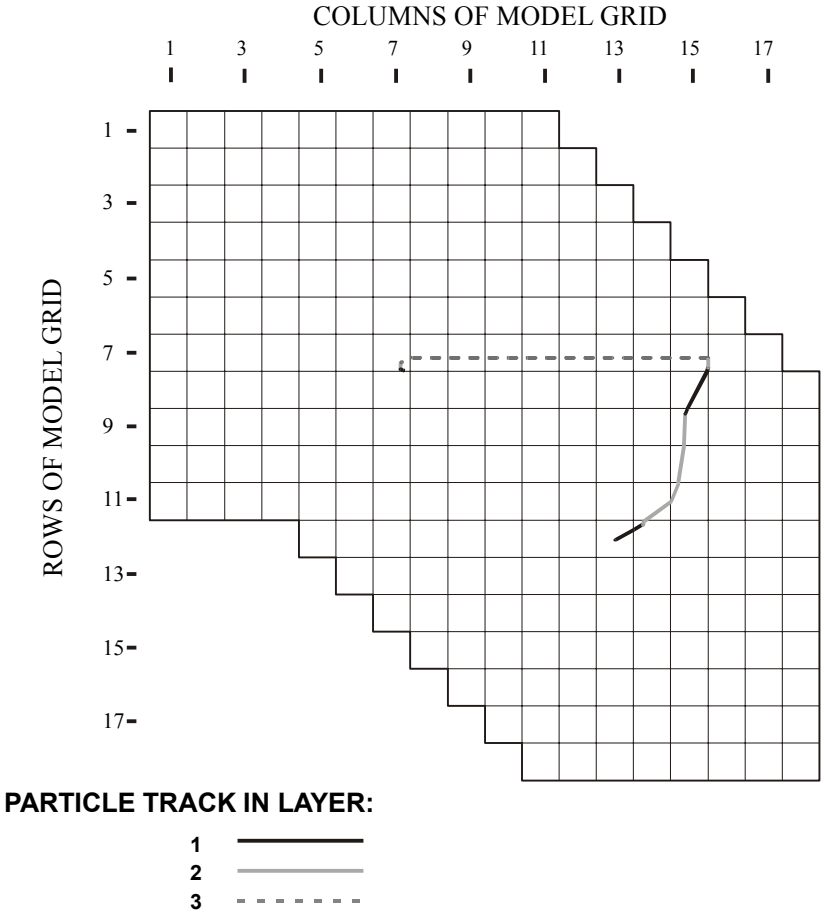

Figure 11. Example of a complex particle track for Test Case 1.

observation. Try to include the observation later in the calibration when the model more accurately represents the actual system.

4. Problem: Unexpected parameter values are estimated when advective-transport observations are included in the parameter estimation.

Discussion: Often, in finding the best fit to the data, the nonlinear regression will estimate parameter values that are unexpected. Re-examine the range of reasonable values and determine whether the unexpected values are unreasonable.

Resolution: If the parameter values are truly unreasonable, see Problem 5.

5. Problem: Unreasonable parameter values are estimated when advective-transport observations are included in the parameter estimation. This problem is also discussed by Hill (1998, p. 13) but is included here because of its prevalence and importance.

Discussion: As demonstrated by Poeter and Hill (1996), the estimation of unreasonable parameter values by regression provides information about likely model accuracy and data accuracy and sufficiency. When advective-transport observations are included in the regression, they may provide information that is different than other types of data and can help identify model error.

Resolution: Parameter estimation merely provides the best fit to the available data with a given model setup. Unreasonable estimated parameter values can be valuable indicators of model error. Scrutinize the sources of available data, including information such as in what season the data were observed, to determine (1) whether the data are correctly interpreted, (2) that the statistic used to calculate the weight correctly represents likely data error, and (3) that the use of a steady-state flow model is adequate. If unreasonable parameter values still cannot be explained, then the conceptual model may be flawed. Re-evaluate the conceptual model and revise the model accordingly.

REFERENCES CITED

Ahmed, S., de Marsily, G., and Talbot, A., 1988, Combined use of hydraulic and electrical properties of an aquifer in a geostatistical estimation of transmissivity: Ground Water, v. 26, no. 1, p. 78-86.

Anderman, E.R., and Hill, M.C., 2000, MODFLOW-2000, the U.S. Geological Survey modular ground-water model – documentation of the hydrogeologic-unit flow (HUF) package: U.S. Geological Survey Open-File Report 00-342, 89 p.

Anderman, E.R., Hill, M.C., and Poeter, E.P., 1996, Two-dimensional advective transport in ground-water flow parameter estimation: Ground Water, v. 34, no. 6, p. 1001-1009.

Carrera, J., and Neuman, S.P., 1986a, Estimation of aquifer parameters under transient and steady state conditions: 1. Maximum likelihood method incorporating prior information: Water Resources Research, v. 22, no. 2, p. 199-210.

_____1986b, Estimation of aquifer parameters under transient and steady state conditions: 2. Uniqueness, stability, and solution algorithms: Water Resources Research, v. 22, no. 2, p. 211-227.

_____1986c, Estimation of aquifer parameters under transient and steady state conditions: 3. Application to synthetic and field data: Water Resources Research, v. 22, no. 2, p. 228-242.

Cheng, J-M., and Yeh, W.W-G., 1992, A proposed quasi-newton method for parameter identification in a flow and transport system: Advances in Water Resources, v. 15, p. 239-249.

Christiansen, H., Hill, M.C., Rosbjerg, D., and Jensen, K.H., 1995, Three-dimensional inverse modeling using heads and concentrations at a Danish landfill, *in* Proceedings of IAHS-IUGG XXI General Assembly, July, 1995, Boulder, Colorado, Wagner, B., and Illangesekare, T., eds.: IAHS Pub No. 27, p. 167-175.

Cooley, R.L., 1982, Incorporation of prior information on parameters into nonlinear regression groundwater flow models, 1, Theory: Water Resources Research, v. 18, no. 4, p. 965- 976.

Cooley, R.L., and Naff, R.L., 1990, Regression modeling of ground-water flow: U.S. Geological Survey Techniques in Water Resources Investigations, Book 3, chapt. B4, 232 p.

Domenico, P.A., and Schwartz, F.W., 1990, Physical and chemical hydrogeology: New York, John Wiley & Sons, 824 p.

Doherty, John, 1994, PEST: Coriander, Australia, Watermark Computing, 122 p.

Doussan, C., Toma, A., Paris, B., Poitevin, G., Ledoux, E., and Detay, M., 1994, Coupled use of thermal and hydraulic head data to characterize river-groundwater exchanges: Journal of Hydrology, v. 153, p. 215-229.

Draper, N.R., and Smith, H., 1981, Applied regression analysis: New York, John Wiley & Sons, 709 p.

Graybill, F.A., 1976, Theory and application of the linear model: Pacific Grove, Wadsworth & Brooks, Calif., 704 p.

Harbaugh, A.W., 1992, A generalized finite-difference formulation for the U.S. Geological Survey modular three-dimensional finite-difference ground-water flow model: U.S. Geological Survey Open-File Report 91-494, 60 p.

Harbaugh, A.W., Banta, E.R., Hill, M.C., and McDonald, M.G., 2000, MODFLOW-2000, the U.S. Geological Survey modular ground-water model – user guide to modularization concepts and the ground-water flow process: U.S. Geological Survey Open-File Report 00-92, 121 p.

Harvey, C.F., and Gorelick, S.M., 1995, Mapping hydraulic conductivity: Sequential conditioning with measurements of solute arrival time, hydraulic head, and local conductivity: Water Resources Research, v. 31, no. 7, p. 1615-1626.

Hess, K.M., Wolf, S.H., and Celia, M.A., 1992, Large-scale natural gradient tracer test in sand and gravel, Cape Cod, Massachusetts 3. Hydraulic conductivity variability and calculated macrodispersivities: Water Resources Research, v. 28, no. 8, p. 2011-2027.

Hill, M.C., 1992, A computer program (MODFLOWP) for estimating parameters of a transient, three-dimensional, ground-water flow model using nonlinear regression: U.S. Geological Survey Open-File Report 91-484, 358 p.

_____1998, Methods and guidelines for effective model calibration: U.S. Geological Survey Water-Resources Investigations Report 98-4005, 90 p.

Hill, M.C., Banta, E.R., Harbaugh, A.W., and Anderman, E.R., 2000, MODFLOW-2000, the U.S. Geological Survey modular ground-water model—User guide to the observation, sensitivity, and parameter-estimation processes and three post-processing programs: U.S. Geological Survey Open-File Report 00-184, 210 p.

Hill, M.C., Cooley, R.L., and Pollock, D.W., 1998, A controlled experiment in ground-water flow model calibration: Ground Water, v. 36, no. 3, p. 520-535.

Hsieh, P.A., and Freckleton, J.R., 1993, Documentation of a computer program to simulate horizontal-flow barriers using the U.S. Geological Survey's modular three-dimensional finite-difference ground-water flow model: U.S. Geological Survey Open-File Report 92-477, 32 p.

Hyndman, D.W., and Gorelick, S.M., 1996, Estimating lithologic and transport properties in three dimensions using seismic and tracer data: The Kesterson aquifer: Water Resources Research, v. 32, no. 9, p. 2659-2670.

Keidser, Allan, and Rosbjerg, Dan, 1991, A comparison of four inverse approaches to ground-water flow and transport parameter identification: Water Resources Research, v. 27, no. 9, p. 2219-2232.

LaVenue, M., Andrews, R.W., and Ramarao, B.S., 1989, Groundwater travel time uncertainty analysis using sensitivity derivatives: Water Resources Research, v. 25, no.7, p. 1551-1566.

LeBlanc, D.R., 1984a, Digital model of solute transport in a plume of sewage contaminated ground water, *in* LeBlanc, D.R., ed., 1984, Movement and fate of solutes in a plume of sewage-contaminated water, Cape Cod, Massachusetts, U.S. Geological Survey Toxic Waste Ground-Water Contamination Program: U.S. Geological Survey Open-File Report 84-475.

_____1984b, Sewage plume in a sand and gravel aquifer, Cape Cod, Massachusetts: U.S. Geological Survey Water-Supply Paper 2218, 28 p.

LeBlanc, D.R., Garabedian, S.P., Hess, K.M., Gelhar, L.W., Quadri, R.D., Stollenwerk, K.G., and Wood, W.W., 1991, Large-scale natural gradient tracer test in sand and gravel, Cape Cod, Massachusetts 1. Experimental design and observed tracer movement: Water Resources Research, v. 27, no. 5, p. 895-910.

McDonald, M.G., and Harbaugh, A.W., 1988, A modular three-dimensional finite difference ground-water flow model: U.S. Geological Survey Techniques in Water Resources Investigations, Book 6, chapt. A1, 548p.

Medina, A., and Carrera, J., 1996, Coupled estimation of flow and solute transport parameters: Water Resources Research, v. 32, no. 10, p. 3063-3076.

Mehl, S., and Hill, M.C., 2000, A comparison of solute-transport solution techniques based on inverse modelling results, *in* Stauffer, F., Kinzelbach, W., Kovar, K., and Hoehn, E., eds., Calibration and reliability in groundwater modelling: Coping with uncertainty: Wallingford, Oxfordshire, UK, IAHS Press, Publication no. 265, p. 205-212.

_____2001, A comparison of solute-transport solution techniques and their effect on sensitivity analysis and inverse modeling results: Ground Water, v. 39, no. 2, p. 300-307.

Poeter, E.P., and Gaylord, D.R., 1990, Influence of aquifer heterogeneity on contaminant transport at the Hanford Site: Ground Water, v., 28, no. 6, p. 900-909.

Poeter, E.P., and Hill, M.C., 1996, Unrealistic parameter estimates in inverse modeling: A problem or benefit for model calibration, *in* Calibration and Reliability in Groundwater Modeling (Proceedings of the ModelCARE 96 Conference held at Golden, Colorado, September 1996): IAHS Publication no. 237, p. 277-285.

_____1998, Documentation of UCODE, A computer code for universal inverse modeling: U.S. Geological Survey Water-Resources Investigations Report 98-4080, 116 p.

Pollock, D.W., 1989, Documentation of computer programs to compute and display pathlines using results from the U.S. Geological Survey modular three-dimensional finite-difference ground-water flow model: U.S. Geological Survey Open-File Report 89-381, 188 p.

_____1994, User's guide for MODPATH/MODPATH-PLOT, version 3: a particle tracking post-processing package for MODFLOW, the U.S. Geological Survey finite-difference ground-water flow model: U.S. Geological Survey Open-File Report 94-464, 249 p.

Strecker, E.W., and Chu, W., 1986, Parameter identification of a ground-water contaminant transport model: Ground Water, v. 24, no. 1, p. 56-72.

Sun, N-Z., 1994, Inverse problems in groundwater modeling: Boston, Klewer, 337 p.

Sun, N-Z., and Yeh, W.W-G., 1990a, Coupled inverse problems in groundwater modeling, 1. Sensitivity analysis and parameter identification: Water Resources Research, v. 26, no. 10, p. 2507-2525.

_____1990b, Coupled inverse problems in groundwater modeling, 2. Identifiability and experimental design: Water Resources Research, v. 26, no. 10, p. 2527-2540.

Sykes, J.F., and Thomson, N.R., 1988, Parameter identification and uncertainty analysis for variably saturated flow: Advances in Water Resources, v. 11, p. 185-191.

Wagner, B.J., and Gorelick, S.M., 1987, Optimal groundwater quality management under parameter uncertainty: Water Resources Research, v. 23, no. 7, p. 1162-1174.

Weiss, R., and Smith, L., 1993, Parameter estimation using hydraulic head and environmental tracer data, *in* Poeter, E.P., Ashlock, S., and Proud, J., eds., Proceedings of the IGWMC

Ground Water Modeling Conference, June 9-12, 1993: Golden, Co., Colorado School of Mines, p. 1-60 to 1-69.

Wexler, E.J., 1992, Analytical solutions for one-, two-, and three-dimensional solute transport in ground-water systems with uniform flow: U.S. Geological Survey Techniques in Water Resources Investigations, book 3, chapt. B7, 190 p.

Woodbury, A.D., and Smith, Leslie, 1988, Simultaneous inversion of hydrogeologic and thermal data, 2. Incorporation of thermal Data: Water Resources Research, v. 24, no. 3, p. 356-372.

Xiang, Y., Sykes, J.F., and Thomson, N.R., 1993, A composite L1 parameter estimator for model fitting in groundwater flow and solute transport simulation: Water Resources Research, v. 29, no. 6, p. 1661-1673.

Yeh, W.W-G., 1986, Review of parameter identification procedures in groundwater hydrology: The inverse problem: Water Resources Research, v. 22, no. 2, p. 95-108.

Zheng, C., 1994, Analysis of particle tracking errors associated with spatial discretization: Ground Water, v. 32, no. 5, p. 821-828.

Zheng, C., and Bennett, G.D., 1995, Applied contaminant transport modeling: theory and practice: New York, Van Nostrand Reinhold, 440 p.

APPENDIX A: ADV2 INPUT AND OUTPUT

The ADV2 Package allows users of MODFLOW-2000 to include advective-transport observations in nonlinear regression. Advective-transport observations as used here are characterized by specified source locations and subsequent particle locations at known times, or specified final locations and previous locations at known times. In the first option, advective transport is simulated forward in time; in the second, it is simulated backward in time. In the text below, the term “initial location” is used to describe the source location for tracking forward in time or the final location for tracking backward in time.

The ADV2 Package also allows the user to specify any number of intermediate observation points along each advective-transport path, thus allowing information about the path of travel to be included in the regression. The observed locations need to be approximated from concentration data derived from either continuous or slug sources. Use of advective-transport observations provides important constraints when calibrating a ground-water flow model and, if applicable, to the development of contaminant transport models.

The ADV2 Package is invoked by specifying a file type "ADV2," a unit number, and the name of the input file in the name file. ITEM 1 of the ADV2 input file contains information about the number of advective-transport observations and flags controlling the particle tracking, which are necessary to dimension the appropriate arrays. ITEM 2 contains arrays of porosity values for each layer and quasi-3D layer in the model grid.

ITEMS 3 and 4 contain observation information. ITEM 3 specifies the number of observation points along the particle track and the initial location. Repetitions of ITEM 4 specify the locations of each of the observed advective-front observations, statistics used to calculate the weights of the observations, and the time of the observation. ITEMS 3 and 4 are repeated as a group for each of the NPTH advective-transport observation paths.

ITEMS 5-7 contain data for the full weight matrix, should a full matrix be used.

ITEMS 1-6 are read in free format; ITEM 7 is read in format FMTIN.

ADV2 Input Instructions

0. [#Text]

Item 0 is optional -- "#" must be in column 1. Item 0 can be repeated multiple times.

1. NPTH NLOC IOUTADV KTFLG KTREV ADVSTP FSNK

2. PRST(NCOL,NROW)

Item 2 is read using the array-reading utility module U2DREL (Harbaugh and others, 2000, p. 86-88. Item 2 is repeated for each model layer and quasi-3D confining unit in the grid. Thus, the number of PRST arrays must equal the number of model layers plus the number of quasi-3D confining beds. These layer variables are read in sequence going down from the top of the system.

3. NPNT SLAY SROW SCOL SLOFF SROFF SCOFF

Items 3-4 are repeated as a group for each advective-transport path to be defined (that is, NPTH times).

4. OBSNAM LAY ROW COL LOFF ROFF COFF XSTAT IXSTAT YSTAT IYSTAT ZSTAT IZSTAT TADV PLOT-SYMBOL

Item 4 is repeated for each advective-transport observation point to be defined along the path (that is, NPNT times).

5. IOWTQAD

Items 6-7 are required if IOWTQAD>0.

6. FMTIN IPRN

7. WTQ(NTT2,NTT2) (format FMTIN)

Explanation of Variables Read by the ADV2 Package

Text - is a character variable (up to 199 characters) that starts in column 2. Any characters can be included in Text. The "#" character must be in column 1. Text is printed when the file is read.

NPTH - is the total number of advective-transport paths that will be used (that is, the total number of repetitions of ITEM 3).

NLOC - is the total number of advective-transport observation locations that will be used (that is, the total number of repetitions ITEM 4).

IOUTADV – is a flag and a unit number.

If IOUTADV > 0, it is the unit number to which the particle-tracking information will be written.

If IOUTADV = 0, particle-tracking information will not be written.

KTFLG – is a flag indicating how the particle-tracking time step is calculated..

If KTFLG = 1, particles are displaced from one cell face to the next, and the time-step length varies.

If KTFLG = 2, particles are displaced using the time steps specified by ADVSTP.

If KTFLG = 3, both of the above are included.

KTREV – is a flag indicating the direction of particle displacement.

If KTREV = 1, particles are displaced in a forward direction.

If KTREV = -1, particles are displaced in a backward direction.

ADVSTP – is the particle-tracking time-step length to be used when KTFLG equals 2 or 3.

FSNK – is a flag and a fraction indicating how weak sinks are treated. Performs identically to Option 3 for terminating pathlines in MODPATH (Pollock, 1989, p. 34).

If FSNK < 0, particles will be discharged at cells with any amount of discharge to boundary conditions.

If FSNK > 0, particles will be discharged at cells where discharge to sinks is larger than the specified fraction of the total inflow to the cell.

PRST – is the porosity of the porous medium represented by a model layer or quasi-3D confining unit.

NPNT – is the number of observation points along the path being defined.

SLAY – is the layer of the initial location.

SROW – is the row of the initial location.

SCOL – is the column of the initial location.

SLOFF – is the layer offset used to locate the initial location within the finite-difference cell (must range between –0.5 at the bottom of the layer and 0.5 at the top of the layer).

SROFF – is the row offset used to locate the initial location within the finite-difference cell (must range between –0.5 and 0.5; see fig. 2 of Hill and others, 2000).

SCOFF – is the column offset used to locate the initial location within the finite-difference cell (must range between –0.5 and 0.5; see fig. 2 of Hill and others, 2000).

OBSNAM – is a string of 1 to 12 nonblank characters used to identify the observation. The identifier need not be unique; however, identification of observations in the output files is facilitated if each observation is given a unique OBSNAM.

LAY – is the layer of the advective-transport observation.

ROW – is the row of the advective-transport observation.

COL – is the column of the advective-transport observation.

LOFF – is the layer offset used to locate the advective-transport observation within the finite-difference cell (must range between –0.5 at the bottom of the layer and 0.5 at the top of the layer).

ROFF – is the row offset used to locate the advective-transport observation within the finite-difference cell (must range between –0.5 and 0.5; see fig. 2 of Hill and others, 2000).

COFF – is the column offset used to locate the advective-transport observation within the finite-difference cell (must range between –0.5 and 0.5; see fig. 2 of Hill and others, 2000).

XSTAT, YSTAT, ZSTAT – are values from which the weights of the observed locations are calculated depending on how IXSTAT, IYSTAT, and IZSTAT are set.

IXSTAT, IYSTAT, IZSTAT – are flags to indicate what XSTAT, YSTAT, and ZSTAT are and how the observation weights are calculated. If the variable STATISTIC represents XSTAT, YSTAT, or ZSTAT and the variable STAT-FLAG represents IXSTAT, IYSTAT, or IZSTAT, respectively, the following definitions apply:

STAT-FLAG = 0, STATISTIC is a scaled variance [L^2], weight = 1/STATISTIC,

STAT-FLAG = 1, STATISTIC is a scaled standard deviation [L], weight = 1/STATISTIC^2, and

STAT-FLAG = 2, STATISTIC is a scaled coefficient of variation [dimensionless], weight = 1/(STATISTIC × Observation value)^2. The observation value is calculated as the distance in the x-, y-, or z-coordinant directions between particle starting position, as defined in input item 3, and the observation positions, as defined in item 4.

TADV – is the time of this advective-front observation, relative to the beginning of the steady-state simulation, in consistent units.

PLOT-SYMBOL – is an integer that is written to output files intended for graphical analysis to allow control of the symbols used to plot data.

IOWTQAD – is a flag indicating whether a full weight matrix will be specified.

If IOWTQAD ≤ 0, a full weight matrix will not be specified and the STATISTIC values in ITEM 4 will be used to calculate weights.

If IOWTQAD > 0, a full weight matrix will be specified.

FMTIN – is the FORTRAN format in which the full weight matrix array values are to be read. The format needs to be enclosed in parentheses and needs to accommodate real numbers.

IPRN -- is a flag identifying the format with which the variance-covariance matrix is printed. If IPRN is less than zero, the matrix is not printed.

Permissible values of IPRN and corresponding formats are:

Output requires more than 80 columns		Output requires 80 columns or less	
IPRN	FORMAT	IPRN	FORMAT
1	10G12.3	6	5G12.3
2	10G12.4	7	5G12.4
3	9G12.5	8	5G12.5
4	8G13.6	9	4G13.6
5	8G14.7	10	4G14.7

WTQ—is an array containing the variance-covariance matrix on advective-transport observations [L^2]. The array is square with dimensions equal to the total number of advective-transport observations (for example, NLOC times two if the tracking is two dimensional or three if the tracking is three dimensional) and for each observation location is entered in the order X, Y, and Z, if applicable. For elements WTQ(I,J), if I ≠ J, WTQ(I,J) is the covariance between observations I and J; if I = J, WTQ(I,J) is the variance of observation I. Note that the

variance-covariance matrix is symmetric, but the entire matrix (upper and lower parts) must be entered.

Example ADV2 input file

The following ADV2 input file is an example of the file used for Test Case 1. The repetitions of item 2 are read using the constant-value option of the UDREL array-reading utility module, which assigns the same value to all cells in a model layer.

```
    2    2   60    1    1    0       0.0                                    ITEM 1
CONSTANT         0.30                                                      ITEM 2, LAYER 1
CONSTANT         0.30                                                      ITEM 2, LAYER 2
CONSTANT         0.30                                                      ITEM 2, LAYER 3
    1    1   14   11  0.5     0.0     0.0                                  ITEM 3, PATH 1
L_6      1   12    5  0.5   -0.09   -0.13   1500.  1   1500.  1    750.  1   5.59e+8    1
                                                                           ITEM 4, PATH 1
    1    1   13   12  0.5     0.0     0.0                                  ITEM 3, PATH 2
C_5      1   10   11 0.48   -0.37   -0.35   1500.  1   1500.  1    750.  1   2.28e+6    1
                                                                           ITEM 4, PATH2
  0                                                                        ITEM 5
```

Output from ADV2

The ADV2 Package fits into the general framework of MODFLOW-2000. Output related to the ADV2 Package is interspersed in the appropriate places throughout the MODFLOW-2000 output. MODFLOW-2000 has the option of creating GLOBAL and LIST output files (Harbaugh and others, 2000, p. 6). If both of the listing files are used, output related to the overall model run is sent to the GLOBAL file, while output from the Ground-Water Flow and Sensitivity Processes is sent to the LIST file, as follows:

- The input information, such as initial position and time and location of the observed position are printed in the GLOBAL file after the flow observation information.
- The simulated row, column, x-, y-, and z-positions, average velocity in a given particle step, and, when the Sensitivity Process is active, the x-, y-, and z-sensitivities to the parameters at each particle-tracking step for each of the parameters, are printed in the LIST file.
- The advective-transport observation residuals, contribution to the sum of the squared weighted residuals, and scaled sensitivities are printed in the GLOBAL file for the first and final parameter-estimation iterations in the appropriate locations with the other observations.
- The advective-transport residuals are included in the list of ordered residuals and normality calculation near the end of the GLOBAL file.

Example ADV2 GLOBAL Output File

An excerpt from the GLOBAL output file for Test Case 1 is included below. The ADV2 package output appears in bold type and three dots (...) indicates omitted output.

```
                                  MODFLOW-2000
      U.S. GEOLOGICAL SURVEY MODULAR FINITE-DIFFERENCE GROUND-WATER FLOW MODEL
                             VERSION 1.0.2 08/21/2000

 This model run produced both GLOBAL and LIST files.  This is the GLOBAL file.

...

 ADV2000 -- OBSERVATION PROCESS (ADVECTIVE TRANSPORT OBSERVATIONS)
 VERSION 2.0, 12/04/2000
 INPUT READ FROM UNIT  27

 NUMBER OF PARTICLES ................................    2
 TOTAL NUMBER OF ADVECTIVE-TRANSPORT OBSERVATIONS ...    2
 OUTPUT UNIT NUMBER FOR ADVECTIVE-TRANSPORT INFO ....   60

 TWO- OR THREE-DIMENSIONAL TRACKING (KTDIM)..........    3
 PARTICLE-TRACKING TIME-STEP FLAG (KTFLG)............    1
 TIME STEP (IF KTFLG>1)..............................  0.0000000
 FORWARD OR BACKWARD PARTICLE TRACKING (KTREV).......    1
 WEAK SINK FLAG/FRACTION.............................  0.0000000

...

   ADVECTIVE-TRANSPORT OBSERVATION DATA
 ----------------------------------------

        POROSITY OF LAYER =  0.300000     FOR LAYER   1

        POROSITY OF LAYER =  0.300000     FOR LAYER   2

        POROSITY OF LAYER =  0.300000     FOR LAYER   3

 3D PARTICLE TRACKING USED IN ALL LAYERS


   PATH # 1 INITIAL LOCATION
 LAYER   ROW    COL    LOFF    ROFF   COFF
-------------------------------------------
    1     14     11   0.500   0.000   0.000

  OBSERVED INTERMEDIATE PATH LOCATION(S)
 OBS #      ID            TIME         LAY ROW COL  LOFF   ROFF   COFF
-----------------------------------------------------------------------
 53- 55 L_6            0.55900000E+09   1  12   5  0.500 -0.090 -0.130

   PATH # 2 INITIAL LOCATION
 LAYER   ROW    COL    LOFF    ROFF   COFF
-------------------------------------------
    1     13     12   0.500   0.000   0.000

  OBSERVED INTERMEDIATE PATH LOCATION(S)
 OBS #      ID            TIME         LAY ROW COL  LOFF   ROFF   COFF
-----------------------------------------------------------------------
 56- 58 C_5             2280000.0       1  10  11  0.480 -0.370 -0.350


SUMMARY OF ADVECTIVE-TRANSPORT OBSERVATIONS:
 OBS #     ID     DIRECTION  TIME           VALUE           WEIGHT          TYPE
-------------------------------------------------------------------------------
   53  L_6            X   0.55900000E+09   6555.0000       2250000.0         1
   54                 Y                    17115.000       2250000.0         1
   55                 Z                    871.62000       562500.00         1
   56  C_5            X    2280000.0       15225.000       2250000.0         1
   57                 Y                    13695.000       2250000.0         1
   58                 Z                    1385.3500       562500.00         1
```

...

OBSERVATION SENSITIVITY TABLE(S) FOR PARAMETER-ESTIMATION ITERATION 1

FOR THE SCALING OF THE SENSITIVITIES BELOW, B IS REPLACED BY
BSCAL (THE ALTERNATE SCALING FACTOR) FOR PARAMETER(S):
HK_1 HK_4 RCH ETM

DIMENSIONLESS SCALED SENSITIVITIES (SCALED BY B*(WT**.5))

OBS #	PARAMETER: OBSERVATION	HK_1	HK_2	HK_3	HK_4	ANIV_12
1	W2L	8.26	19.2	-11.8	-706.	8.24
2	WL2	8.19	12.5	-9.67	-608.	8.44
3	WL2	9.06	-18.9	-2.11	-227.	10.1
4	WL4	2.79	5.54	-2.62	-469.	1.19
5	WL4	8.33	21.4	-11.2	-683.	7.76
6	WL4	8.88	-15.6	-2.92	-285.	9.89
7	WL4	6.51	-18.9	-1.90	-212.	10.2
8	WL5	10.1	12.2	-3.33	-0.139E+04	-0.544
9	WL6	3.17	1.14	-0.567	259.	-1.46
10	WL6	21.6	20.0	-0.498	-22.9	-6.32
11	WL6	21.7	17.6	0.154	19.7	-6.89
12	WL6	4.92	-18.2	-2.13	-252.	10.1
13	WL6	3.96	-19.0	-1.74	-199.	10.3
14	WL6	3.49	-19.0	-1.65	-191.	10.3
15	WL8	4.94	-6.14	4.55	978.	-2.97
16	WL8	14.9	2.83	-0.665	800.	0.226
17	WL8	25.7	-1.40	-0.190	2.68	-2.31
18	WL8	8.97	-24.9	0.132	-0.115E+04	8.88
19	WL8	1.61	-28.6	-2.14	-246.	11.1
20	WL8	2.43	-19.0	-1.60	-186.	10.2
21	WL9	10.6	-3.35	1.46	0.139E+04	-0.904E-01
22	WL10	15.0	-1.57	-0.752	0.145E+04	0.975
23	WL10	22.9	2.20	-2.38	715.	-1.93
24	WL10	14.7	-12.6	-0.296	-200.	2.00
25	WL10	0.303	-47.6	-3.98	-316.	10.8
26	WL10	-1.54	-31.7	-1.91	-207.	11.9
27	WL10	0.540E-01	-10.5	-0.847	-97.3	5.08
28	WL11	8.01	-8.33	5.36	0.131E+04	-1.52
29	WL12	10.3	-11.4	0.491E-01	300.	-0.432
30	WL12	1.24	-40.7	-1.14	-548.	7.63
31	WL12	-2.13	-68.3	-3.62	-276.	12.3
32	WL12	-1.63	-20.7	-1.15	-130.	7.11
33	WL13	-1.96	-66.3	-5.37	-338.	11.6
34	WL13	-1.81	-38.9	-1.52	-156.	10.6
35	WL14	3.87	-29.2	-0.952	-228.	2.93
36	WL14	-0.796	-53.0	-2.43	-517.	9.59
37	WL14	-1.01	-16.1	-0.606	-82.0	3.87
38	WL15	-0.250	-7.05	2.63	-33.0	1.10
39	WL16	0.912	-28.9	-0.965	-178.	3.09
40	WL16	-1.15	-16.8	-0.560	-83.9	4.10
41	WL18	0.351	-23.2	-0.782	-84.0	2.53
42	WL18	-1.11	-16.3	-0.464	-81.6	3.90
43	DRN1	-0.561	-0.377	0.977E-02	0.270	0.135
44	DRN1	-0.468E-02	0.734	0.613E-01	4.88	-0.167
45	DRN1	0.147	3.53	0.189	15.1	-0.834
46	DRN1	0.171	4.84	-1.80	22.6	-0.756
47	DRN1	0.123	8.12	-2.29	28.3	-0.537
48	GHB1	-0.217	-0.632	0.294	18.0	-0.212
49	GHB2	-0.211	0.457	0.495E-01	5.39	-0.244
50	GHB3	-0.181	0.256	0.481E-01	5.34	-0.240
51	GHB4	-0.143	0.188	0.462E-01	5.33	-0.238
52	GHB5	-0.551	1.92	-2.22	15.6	0.261
53	**L_6**	**0.968**	**2.14**	**-4.92**	**119.**	**-0.681E-01**
54	**L_6**	**0.708**	**0.758**	**-2.36**	**30.5**	**0.500E-01**
55	**L_6**	**-0.761E-08**	**-0.127E-07**	**-0.990E-08**	**-0.950E-06**	**0.747E-08**
56	**C_5**	**0.178E-01**	**0.184**	**-0.516E-01**	**-2.32**	**-0.429E-01**
57	**C_5**	**-0.680E-01**	**-0.213**	**0.194**	**1.11**	**-0.664E-01**
58	**C_5**	**0.703E-02**	**-0.361E-01**	**-0.464E-01**	**-3.85**	**0.256E-01**
	COMPOSITE SCALED SENSITIVITIES ((SUM OF THE SQUARED VALUES)/ND)**.5	8.09	22.0	3.20	498.	6.16

Example ADV2 LIST Output File

An excerpt from the LIST output file for Test Case 1 is included below. The ADV2 package output appears in bold type and three dots (...) indicates omitted output.

```
                                  MODFLOW-2000
      U.S. GEOLOGICAL SURVEY MODULAR FINITE-DIFFERENCE GROUND-WATER FLOW MODEL
                              VERSION 1.0.2 08/21/2000

 This model run produced both GLOBAL and LIST files.  This is the LIST file.

...

      ENTERING PARTICLE TRACKING ROUTINE (OBS1ADV2P)
 -----------------------------------------------------
 SUBROUTINE (OBS1ADV2P) IS HARDWIRED WITH THE FOLLOWING OPTIONS:
 LINEAR VELOCITY INTERPOLATION (SOBS1ADV2L)
 SEMI-ANALYTICAL PARTICLE TRACKING (SOBS1ADV2S)


 ADVECTIVE-TRANSPORT OBSERVATION NUMBER   1
         PARTICLE TRACKING LOCATIONS AND TIMES:
 LAYER ROW  COL   X-POSITION      Y-POSITION      Z-POSITION        TIME
-------------------------------------------------------------------------------
    1   14   11   15750.000       20250.000       1375.3900       0.0000000
    1   15   11   15308.220       21000.000       1282.8600       34107204.
    1   15   10   15000.000       21345.236       1242.5200       57161892.
    1   15    9   13500.000       22119.861       1241.0699      0.13500235E+09
    1   15    8   12000.000       21465.570       1239.2100      0.18821832E+09
    1   14    8   11324.291       21000.000       1183.1700      0.21663123E+09
    1   14    7   10500.000       19695.488       1117.5100      0.30001466E+09
    1   13    7   10279.665       19500.000       1063.0500      0.32152035E+09
    1   13    6   9000.0000       18273.896       1000.3800      0.45110346E+09
    1   12    6   8711.9150       18000.000       949.88000      0.48301728E+09
.................................................................................
OBS #  53- 55     OBS NAME: L_6
    1   12    6   7824.0649       17333.936       949.88000      0.55900000E+09
.................................................................................
END OF PATH    1 REACHED
 AVERAGE PARTICLE VELOCITY ALONG PATH:  0.18989491E-04


 ADVECTIVE-TRANSPORT OBSERVATION NUMBER   2
         PARTICLE TRACKING LOCATIONS AND TIMES:
 LAYER ROW  COL   X-POSITION      Y-POSITION      Z-POSITION        TIME
-------------------------------------------------------------------------------
    1   13   12   17250.000       18750.000       1513.5300       0.0000000
    1   12   12   17054.016       18000.000       1156.1790       595736.12
    1   11   12   16926.127       16500.000       1044.6531       1096153.0
    1   10   12   16828.191       15000.000       1007.6937       1374752.0
    1   10   11   16500.000       13833.491       933.09253       1572575.4
.................................................................................
OBS #  56- 58     OBS NAME: C_5
    1   10   11   15578.235       13821.779       1030.0319       2280000.0
.................................................................................
END OF PATH    2 REACHED
 AVERAGE PARTICLE VELOCITY ALONG PATH:  0.26350063E-02


 ALL PARTICLES MOVED EXITING (OBS1ADV2P)

...

 ADVECTIVE-TRANSPORT OBSERVATIONS
                          OBSERVED   CALCULATED             WEIGHT  WEIGHTED
  OBS#   ID               LOCATION    LOCATION  RESIDUAL     **0.5  RESIDUAL

    53 L_6          X =   0.656E+04  0.782E+04 -0.127E+04  0.667E-03 -0.846
    54 L_6          Y =   0.171E+05  0.173E+05  -219.      0.667E-03 -0.146
    55 L_6          Z =    872.       950.      -78.3      0.133E-02 -0.104
```

```
   56 C_5          X =   0.152E+05  0.156E+05  -353.      0.667E-03 -0.235
   57 C_5          Y =   0.137E+05  0.138E+05  -127.      0.667E-03 -0.845E-01
   58 C_5          Z =   0.139E+04  0.103E+04   355.      0.133E-02  0.474
 STATISTICS FOR ADVECTIVE-TRANSPORT RESIDUALS :
 MAXIMUM WEIGHTED RESIDUAL  : 0.474E+00 OBS#     58
 MINIMUM WEIGHTED RESIDUAL  :-0.846E+00 OBS#     53
 AVERAGE WEIGHTED RESIDUAL  :-0.157E+00
 # RESIDUALS >= 0. :      1
 # RESIDUALS < 0.  :      5
 NUMBER OF RUNS  :    2  IN    6 OBSERVATIONS

 SUM OF SQUARED WEIGHTED RESIDUALS
 (ADVECTIVE-TRANSPORT OBSERVATIONS ONLY)   1.0350

...

 SOLVING PARAMETER SENSITIVITY FOR HK_1
 SUM OF POSITIVE RATES= 2.79796E+04    SUM OF NEGATIVE RATES= 2.79796E+04
              PERCENT DISCREPANCY=    0.00


       ENTERING PARTICLE TRACKING ROUTINE (OBS1ADV2P)
 ----------------------------------------------------------
 SUBROUTINE (OBS1ADV2P) IS HARDWIRED WITH THE FOLLOWING OPTIONS:
 LINEAR VELOCITY INTERPOLATION (SOBS1ADV2L)
 SEMI-ANALYTICAL PARTICLE TRACKING (SOBS1ADV2S)


 ADVECTIVE-TRANSPORT OBSERVATION NUMBER   1     PARAMETER #:   1 TYPE: HK
  PARTICLE TRACKING LOCATIONS, TIMES, AND SENSITIVITIES:

 SENSITIVITIES ARE SCALED USING ALTERNATE SCALING FACTOR
 LAYER ROW  COL  X-SENSIVITY     Y-SENSIVITY     Z-SENSIVITY        TIME
-------------------------------------------------------------------------------
    1   14   11   0.0000000       0.0000000       0.0000000       0.0000000
    1   15   11  0.42450000E-01 -0.33535536E-01 -0.45237969E-09   34107204.
    1   15   10  0.88220626E-01 -0.46312317E-01 -0.47110960E-09   57161892.
    1   15    9  0.39392111     -0.41777629E-01 -0.51601184E-09  0.13500235E+09
    1   15    8  0.74690485      0.71606919E-01 -0.80430251E-09  0.18821832E+09
    1   14    8  0.49031159      0.19152847     -0.17369635E-08  0.21663123E+09
    1   14    7  0.77294344      0.27135566     -0.33723835E-08  0.30001466E+09
    1   13    7  0.69353050      0.34577930     -0.34308676E-08  0.32152035E+09
    1   13    6  0.93518907      0.53729993     -0.37910715E-08  0.45110346E+09
    1   12    6  0.79364455      0.70259136     -0.38375525E-08  0.48301728E+09
.................................................................................
OBS #  53- 55     OBS NAME: L_6
    1   12    6  0.96761692      0.70805061     -0.38059098E-08  0.55900000E+09
.................................................................................
END OF PATH    1 REACHED
 AVERAGE PARTICLE VELOCITY ALONG PATH:  0.18989491E-04


 ADVECTIVE-TRANSPORT OBSERVATION NUMBER   2     PARAMETER #:   1 TYPE: HK
  PARTICLE TRACKING LOCATIONS, TIMES, AND SENSITIVITIES:
     SENSITIVITIES ARE SCALED BY B*(WT**.5)
 LAYER ROW  COL  X-SENSIVITY     Y-SENSIVITY     Z-SENSIVITY        TIME
-------------------------------------------------------------------------------
    1   13   12   0.0000000       0.0000000       0.0000000       0.0000000
    1   12   12  0.31437038E-02 -0.17931741E-01  0.11281397E-03   595736.12
    1   11   12  0.13406117E-01 -0.96344128E-01  0.26992458E-03   1096153.0
    1   10   12  0.24420679E-01 -0.16178754      0.31196006E-03   1374752.0
    1   10   11  0.38425937E-01 -0.16746560      0.32050992E-03   1572575.4
.................................................................................
OBS #  56- 58     OBS NAME: C_5
    1   10   11  0.17798102E-01 -0.67955017E-01  0.35146901E-02   2280000.0
.................................................................................
END OF PATH    2 REACHED
 AVERAGE PARTICLE VELOCITY ALONG PATH:  0.26350063E-02


 ALL PARTICLES MOVED EXITING (OBS1ADV2P)
```

APPENDIX B: DERIVATION OF SENSITIVITY EQUATIONS

Calculation of Particle Location

The x-location of a particle at any given time equals the initial location plus the cumulative displacement up to that time. At the end of particle-tracking time step t, the x-location of the particle equals:

$$x_p^t = x_p^0 + \sum_{t=1}^{NPSTP} \Delta x_p^t \tag{B1}$$

where

x_p^0 is the starting position of the observed path of advective transport and the particle [L],
t is the particle time-step counter
$NPSTP$ is the number of previous particle time steps, and
Δx_p^t is the particle x-displacement for time step t [L].

When the particle is in the cell at row i, column j, and layer k, particle displacement over time step Δt is calculated using the semi-analytical exponential particle-tracking method (Pollock, 1989) as:

$$\Delta x_p^t = x_p^t - x_p^{t-1} = \frac{1}{A_{x_{i,j,k}}}\left(v_{xp}^{t-1} e^{A_{x_{i,j,k}}\Delta t} - v_{x_{i,j-1/2,k}}\right) \tag{B2}$$

$$A_{x_{i,j,k}} = \frac{v_{x_{i,j+1/2,k}} - v_{x_{i,j-1/2,k}}}{\Delta r_j} \tag{B3}$$

where

v_{xp}^{t-1} is the linearly-interpolated x-velocity of particle p at time t-1 [L/T],
Δt is the length of time step t [T],
$v_{x_{i,j-1/2,k}}$ is the x-velocity at the left-hand face of the cell at row i, column j, and layer k [L/T],
$v_{x_{i,j+1/2,k}}$ is the x-velocity at the right-hand face of the cell at row i, column j, and layer k [L/T], and
Δr_j is the cell width of column j [L].

To interpolate velocity linearly for any point p within cell i,j,k, it is assumed that the x-component of velocity, v_{xp}, is dependent only on its location along the x-axis relative to the location of the two cell faces perpendicular to the x-axis, and is independent of the y- or z-position within the

cell. Thus, the x-component of the velocity will be continuous in the x-direction and discontinuous in the other directions. The x-component of the velocity for any point *p* in cell *i,j,k* is given by Pollock (1989) as:

$$v_{xp}^{t-1} = A_{x_{i,j,k}}\left(x_p^{t-1} - x_{i,j-1/2,k}\right) + v_{x_{i,j-1/2,k}} \tag{B4}$$

where

v_{xp}^{t-1} is the x-component of velocity at point $x_p(t-1)$ [L/T],

x_p^{t-1} is the x-position of the particle at time step *t*-1, and is used to interpolate velocity to move the particle during time step *t* [L],

$x_{i,j-1/2,k}$ is the x-position of the left-hand cell face [L], and

$v_{x_{i,j-1/2,k}}$ is the velocity at the left-hand cell face [L/T].

The cell-face velocities are calculated as the flow rate through the cell face divided by the effective area of flow and are dependent on the change in head across the cell face and the hydraulic conductivity and porosity of the material. Derivations of the cell-face velocities and their sensitivities are given below.

Sensitivity of Particle Location

To calculate the sensitivity of particle location to a parameter, *b*, first note that, because x_p^0 is defined by the user, $\frac{\partial x_p^0}{\partial b}$ is equal to zero. Then, because differentiation and summation are linear, the sensitivity of the particle location to a parameter is calculated as the sum of the sensitivities of each of the particle displacements:

$$\frac{\partial x_p^0}{\partial b} = \sum_{t=1}^{NPSTP} \frac{\partial \Delta x_p^0}{\partial b} \tag{B5}$$

Sensitivity of Semi-Analytical Particle Displacement

The derivative of equation B2 with respect to a parameter *b* is:

$$\frac{\partial \Delta x_p^t}{\partial b} = -\frac{\frac{\partial A_{x_{i,j,k}}}{\partial b}}{A_{x_{i,j,k}}^2}\left\{v_{xp}^{t-1} e^{A_{x_{i,j,k}}\Delta t} - v_{x_{i,j-1/2,k}}\right\}$$
$$+\frac{1}{A_{x_{i,j,k}}}\left\{\frac{\partial v_{xp}^{t-1}}{\partial b} e^{A_{x_{i,j,k}}\Delta t} + \frac{\partial A_{x_{i,j,k}}}{\partial b}\Delta t v_{xp}^{t-1} e^{A_{x_{i,j,k}}\Delta t} - \frac{\partial v_{x_{i,j-1/2,k}}}{\partial b}\right\} \quad \text{(B6)}$$

where $\frac{\partial \Delta t}{\partial b}$ equals zero because time is an independent variable.

Sensitivity of Linear Velocity Interpolation Coefficient

The derivative of $A_{x_{i,j,k}}$ in equation B3 with respect to any parameter *b* is given as:

$$\frac{\partial A_{x_{i,j,k}}}{\partial b} = \frac{1}{\Delta r_j}\left(\frac{\partial v_{x_{i,j+1/2,k}}}{\partial b} - \frac{\partial v_{x_{i,j-1/2,k}}}{\partial b}\right) \quad \text{(B7)}$$

Calculation of Linearly Interpolated Velocity and Sensitivity

The sensitivity of the x-component of the interpolated velocity at any point *p* of equation B4 with respect to a parameter *b* is:

$$\frac{\partial v_{xp}^{t-1}}{\partial b} = \frac{\partial A_{x_{i,j,k}}}{\partial b}\left(x_p^{t-1} - x_{i,j-1/2,k}\right) + A_{x_{i,j,k}}\frac{\partial x_p^{t-1}}{\partial b} + \frac{\partial v_{x_{i,j-1/2,k}}}{\partial b} \quad \text{(B8)}$$

Calculation of Horizontal Cell-Face Velocities and Sensitivities

The velocity on the left x-face of cell *i,j,k* is defined as the flow rate through the cell face divided by the effective area of flow:

$$v_{x_{i,j-1/2,k}} = \frac{2Q_{x_{i,j-1/2,k}}}{n_{i,j,k}\Delta c_i\left(l_{i,j-1,k} + l_{i,j,k}\right)} \quad \text{(B9)}$$

where

$v_{x_{i,j-1/2,k}}$ is the velocity on face *i,j-½,k* [L/T],

$Q_{x_{i,j-1/2,k}}$ is the cell-face flow rate [L^3/T],

Δc_i is the cell width of row *i* [L],

$n_{i,j,k}$ is the effective porosity of cell *i,j,k*, and

$l_{i,j,k}$ is the saturated thickness of unconfined cell *i,j,k* or thickness of confined cell *i,j,k* [L].

The cell-face velocities are calculated using an average saturated thickness, instead of the single-cell saturated thickness used in MODPATH, because the original method produces discontinuities in velocity, and thus in sensitivity, at cell boundaries. The cell-face flow rate equals conductance multiplied by the head difference across the cell face (McDonald and Harbaugh, 1988, p. 2-12). For the left cell face *j*-1/2:

$$Q_{x_{i,j-1/2,k}} = CR_{i,j-1/2,k}(h_{i,j-1,k} - h_{i,j,k}) \tag{B10}$$

$$CR_{i,j-1/2,k} = 2\Delta c_i \frac{T_{i,j-1,k}T_{i,j,k}}{T_{i,j-1,k}\Delta r_j + T_{i,j,k}\Delta r_{j-1}} \tag{B11}$$

where

$CR_{i,j-1/2,k}$ is the conductance in the row direction for the material between the center of adjacent cells *i,j*-1,*k* and *i,j,k* [L^2/T],

$h_{i,j,k}$ is the head in cell *i,j,k* [L],

Δr_j is the cell width of column *j* [L],

Δc_i is the cell width of row *i* [L], and

$T_{i,j,k}$ is the transmissivity of cell *i,j,k* [L^2/T].

Substituting equation B10 into equation B9 produces:

$$v_{x_{i,j-1/2,k}} = \frac{2CR_{i,j-1/2,k}(h_{i,j-1,k} - h_{i,j,k})}{n_{i,j,k}\Delta c_i\left(l_{i,j-1,k} + l_{i,j,k}\right)} \tag{B12}$$

The partial derivative of the left cell-face velocity with respect to a parameter *b* is:

$$\frac{\partial v_{x_{i,j-1/2,k}}}{\partial b} = \tag{B13}$$

$$\frac{2}{n_{i,j,k}\Delta c_i}\left[\begin{array}{l}\dfrac{\partial CR_{i,j-1/2,k}}{\partial b}\dfrac{(h_{i,j-1,k}-h_{i,j,k})}{(l_{i,j-1,k}+l_{i,j,k})}+ \\ CR_{i,j-1/2,k}\left(\dfrac{(l_{i,j-1,k}+l_{i,j,k})\left(\dfrac{\partial h_{i,j-1,k}}{\partial b}-\dfrac{\partial h_{i,j,k}}{\partial b}\right)-(h_{i,j-1,k}-h_{i,j,k})\left(\dfrac{\partial h_{i,j-1,k}}{\partial b}+\dfrac{\partial h_{i,j,k}}{\partial b}\right)}{(l_{i,j-1,k}+l_{i,j,k})^2}\right)\end{array}\right]$$

where the sensitivities of the conductance term and of the hydraulic heads to the parameters are calculated by MODFLOW-2000 using the sensitivity-equation method. Equation B13 shows that there are two components that influence the velocity sensitivity. First, there is the effect due to the sensitivity of the cell hydraulic conductivity to the parameter of interest $\frac{\partial CR_{i,j-1/2,k}}{\partial b}$, which will be zero if the parameter is not included in $CR_{i,j-1/2,k}$. Second, there is the effect of the head sensitivity to the parameter $\frac{\partial h_{i,j-1,k}}{\partial b}$ or $\frac{\partial h_{i,j,k}}{\partial b}$, which may influence the sensitivities in each cell of the grid due to the change in the head distribution from a change in a parameter value anywhere in the grid. The velocity in every cell, therefore, may be at least somewhat sensitive to all of the parameters.

Calculation of Vertical Cell-Face Velocity and Sensitivity at the Top of the Top Layer

The vertical velocity at the top of the top layer is calculated using the net flux across the top of the layer into or out of the model. Taking velocity in the upward direction as being positive, the velocity $v_{z_{i,j,k-1/2}}$ can be expressed as:

$$v_{z_{i,j,k-1/2}} = -\frac{W_{i,j,k}}{n_{i,j,k}} \tag{B14}$$

where

$W_{i,j,k}$ is the net flux across the top of cell *i,j,k* [L/T], and

$n_{i,j,k}$ is the porosity of layer *k*.

The sensitivity of the vertical velocity at the top of the top layer given by equation B14 is obtained by taking the derivative with respect to a general parameter *b*:

$$\frac{\partial v_{z_{i,j,k-1/2}}}{\partial b} = -\frac{1}{n_{i,j,k}} \frac{\partial W_{i,j,k}}{\partial b} \tag{B15}$$

When more than one type of boundary contributes to the flux across the top of the top layer, then, because the differential and summation functions are linear, the sensitivity of the velocity is equal to the sum of the sensitivity of each of the components.

Calculation of Vertical Cell-Face Velocity and Sensitivities Between Layers

Vertical conductance is used to calculate the flux between two layers using the head difference across the layer:

$$Q_{i,j,k+1/2} = CV_{i,j,k+1/2}\left(h_{i,j,k+1} - h_{i,j,k}\right) \tag{B16}$$

The vertical conductance between two model layers is calculated as:

$$CV_{i,j,k+1/2} = \frac{\Delta r_j \Delta c_i}{\frac{l_{i,j,k}}{2K_{z_{i,j,k}}} + \frac{l_{i,j,k+1}}{2K_{z_{i,j,k}}}} \tag{B17}$$

where

$K_{z_{i,j,k}}$ is the vertical hydraulic conductivity of cell *i,j,k* [L/T], and

$l_{i,j,k}$ is the thickness of layer *k* [L],

and the vertical conductance between two model layers separated by a quasi-3D confining unit is calculated as:

$$CV_{i,j,k+1/2} = \frac{\Delta r_j \Delta c_i}{\frac{l_{i,j,k}}{2K_{z_{i,j,k}}} + \frac{l_{i,j,k+1/2}}{K_{z_c}} + \frac{l_{i,j,k+1}}{2K_{z_{i,j,k+1}}}} \tag{B18}$$

where

K_{z_c} is the vertical hydraulic conductivity of the confining layer [L/T], and

$l_{i,j,k+1/2}$ is the thickness of the confining layer [L].

Vertical velocity is calculated from the flow between layers by dividing equation B16 by the effective area of flow. If the particle is in model layer *k*, the velocity is:

$$v(k)_{z_{i,j,k+1/2}} = \frac{CV_{i,j,k+1/2}\left(h_{i,j,k+1} - h_{i,j,k}\right)}{n_{i,j,k}\Delta r_j \Delta c_i} \tag{B19a}$$

and if the particle is in model layer *k*+1 the velocity is:

$$v(k+1)_{z_{i,j,k+1/2}} = \frac{CV_{i,j,k+1/2}\left(h_{i,j,k+1} - h_{i,j,k}\right)}{n_{i,j,k+1}\Delta r_j \Delta c_i} \tag{B19b}$$

The sensitivity of the velocities in equation B19 are:

$$\frac{\partial v(k)_{z_{i,j,k+1/2}}}{\partial b} = \tag{B20a}$$

$$\frac{1}{n_{i,j,k}\Delta r_j \Delta c_i}\left[\frac{\partial CV_{i,j,k+1/2}}{\partial b}\left(h_{i,j,k+1} - h_{i,j,k}\right) + CV_{i,j,k+1/2}\left(\frac{\partial h_{i,j,k+1}}{\partial b} - \frac{\partial h_{i,j,k}}{\partial b}\right)\right]$$

$$\frac{\partial v(k+1)_{z_{i,j,k+1/2}}}{\partial b} = \tag{B20b}$$

$$\frac{1}{n_{i,j,k+1}\Delta r_j \Delta c_i}\left[\frac{\partial CV_{i,j,k+1/2}}{\partial b}\left(h_{i,j,k+1} - h_{i,j,k}\right) + CV_{i,j,k+1/2}\left(\frac{\partial h_{i,j,k+1}}{\partial b} - \frac{\partial h_{i,j,k}}{\partial b}\right)\right]$$

With the exception of the different porosity terms and the absence of the saturated thickness term, equation B20 is similar to the horizontal cell-face sensitivity in equation B13.

Calculation of Particle Displacement and Sensitivity in Layers Separated by a Quasi-3D Confining Unit

If adjacent layers are being represented as having a quasi-3D confining unit separating them, then the particle tracking and calculation of sensitivities are more complicated. It is assumed that flow through a quasi-3D confining unit is vertical. In this case, the x- and y-locations of the particle, and thus their sensitivities, will not change as the particle travels through the confining unit. Because of continuity of flow, the velocity in the model layers above and below the confining unit can be calculated using equations B19 above. Particle displacement in the model layers is calculated using exponential particle tracking. The velocity in the confining unit is calculated as in equation B19, but using the porosity of the confining unit $n_{i,j,c}$, as:

$$v_{z_{i,j,c}} = \frac{CV_{i,j,k+1/2}\left(h_{i,j,k+1} - h_{i,j,k}\right)}{n_{i,j,c}\Delta r_j \Delta c_i} \tag{B21}$$

The time that it takes the particle to travel through the confining unit is calculated using Euler-integration particle tracking:

$$\Delta t_z = \frac{l_{i,j,k+1/2} n_{i,j,c} \Delta r_j \Delta c_i}{CV_{i,j,k+1/2}\left(h_{i,j,k+1} - h_{i,j,k}\right)} \tag{B22}$$

The sensitivity of the vertical velocity within a quasi-3D confining unit of equation B21 is:

$$\frac{\partial v_{z_{i,j,c}}}{\partial b} = \frac{1}{n_{i,j,c}\Delta r_j \Delta c_i}\left[\frac{\partial CV_{i,j,k+1/2}}{\partial b}\left(h_{i,j,k+1} - h_{i,j,k}\right) + CV_{i,j,k+1/2}\left(\frac{\partial h_{i,j,k+1}}{\partial b} - \frac{\partial h_{i,j,k}}{\partial b}\right)\right] \tag{B23}$$

Then the sensitivity of the change in the z-location of the particle to a parameter *b* is calculated as:

$$\frac{\partial \Delta z}{\partial b} = \frac{\partial v_{z_{i,j,k+1/2}}}{\partial b}\Delta t_z = \frac{\partial v_{z_{i,j,k+1/2}}}{\partial b}\frac{l_{i,j,k+1/2} n_{i,j,c} \Delta r_j \Delta c_i}{CV_{i,j,k+1/2}\left(h_{i,j,k+1} - h_{i,j,k}\right)} \tag{B24}$$

where, because time is an independent variable, the sensitivity of the time step size $\frac{\partial \Delta t_z}{\partial b}$ is zero.

Correction of Vertical Position for Distorted Grids

The corrected position is calculated using the uncorrected position and thickness and bottom elevation of the respective cells. When the particle moves from column *j* to column *j*+1, for example, the correction is calculated as:

$$z^{t}_{p_{corrected}} = z_{bot_{i,j+1,k}} + \frac{z^{t}_{p_{uncorrected}} - z_{bot_{i,j,k}}}{l_{i,j,k}} l_{i,j+1,k} \tag{B25}$$

where

$z^{t}_{p_{corrected}}$ is the corrected vertical position of the particle at time-step *t*,

$z^{t}_{p_{uncorrected}}$ is the uncorrected vertical position of the particle at time-step *t*, and

$z_{bot_{i,j,k}}$ is the elevation of the bottom of cell *i,j,k*.

APPENDIX C: PROGRAM DESCRIPTION

Advective-transport observations are included in a parameter-estimation iteration subsequent to the calculation of the heads by calling the module OBS1ADV2P from the main program unit. When the advective-transport observation process is active, subroutine OBS1ADV2P is called to track particles by (1) initializing the coordinates of the particle at the starting position of the observed path of advective transport, (2) tracking the particle through the grid using equations B1 and B2. If the Sensitivity Process is active, OBS1ADV2P is called a second time to calculate sensitivities using equations B5 and B6. OBS1ADV2P calls SOBS1ADV2L to calculate the linearly-interpolated velocity from the cell-face velocities. OBS1ADV2P then calls SOBS1ADV2S to calculate the semi-analytical particle displacement. When the observation time is reached, the particle tracking is stopped. If the Parameter-Estimation Process is active, the final x-, y-, and z-locations and the sensitivities of those locations to the parameters are used by the modified Gauss-Newton optimization method in addition to the head and flow observations to update the parameter values.

Description of ADV2 Subroutines

A brief description of the subroutines included in the ADV2 Package is given below.

Subroutine name	Subroutine function
OBS1ADV2AL	Allocates array storage for advective-transport observations. Calls utility subroutines URDCOM and URWORD to read and parse the first line of the input file.
OBS1ADV2RP	Reads, checks, prints, and stores information from the ADV2 input file. Calls utility subroutines URDCOM and URWORD to read and parse the lines of the input file. Calls UARRSUBPRW to print the full weight matrix.
OBS1ADV2P	Controls tracking of particles. Calls subroutines SOBS1ADV2WR, SOBS1ADV2L, SOBS1ADV2S, SOBS1ADV2UP, and SOBS1ADV2CC.

SOBS1ADV2L	Calculates the linearly-interpolated velocity at any point within a cell from the cell-face velocities and calculates sensitivity of that velocity to the parameters. Calls subroutines SOBS1ADV2LPF and SOBS1ADV2HUF.
SOBS1ADV2LPF	Computes conductance sensitivities for the LPF package. Calls subroutines SSEN1LPF1CH (calculates sensitivity of horizontal conductance to parameter), SSEN1HFB6MD (calculates correction for horizontal flow barrier), and SSEN1LPF1CV (calculates sensitivity of vertical conductance to parameter).
SOBS1ADV2HUF	Computes conductance sensitivities for the HUF package. Calls subroutines SSEN1HUF1THK (determines thickness of hydrogeologic unit in current cell), SSEN1HUF1CH (calculates sensitivity of horizontal conductance to parameter), SSEN1HFB6MD (calculates correction for horizontal flow barrier), and SSEN1HUF1CV (calculates sensitivity of vertical conductance to parameter).
SOBS1ADV2S	Calculates the semi-analytical particle displacement and sensitivity to parameters.
SOBS1ADV2O	Prints information about the advective-transport observation residuals.
SOBS1ADV2WR	Writes particle-tracking summary information to the GLOBAL output file and IOUTT2 file, if specified.
SOBS1ADV2UP	Updates the position of the particle given the displacements calculated in SOBS1ADV2S.
SOBS1ADV2CC	Tracks a particle through a confining unit. Calls subroutine SOBS1ADV2WR.